Pharmacological Research 139 (2019) 471–488

Contents lists available at ScienceDirect

Pharmacological Research

journal homepage: www.elsevier.com/locate/yphrs

Invited Review

Cyclin-dependent protein serine/threonine kinase inhibitors as anticancer drugs

Robert Roskoski Jr.

Blue Ridge Institute for Medical Research, 3754 Brevard Road, Suite 116, Box 19, Horse Shoe, NC, 28742-8814, United States

ARTICLE INFO

Chemical compounds studied in this article:
Abemaciclib (PubMed CID: 46220502)
Alvocidib (PubMed CID: 5287969)
AT7519M (PubMed CID: 23657720)
Dinaciclib (PubMed CID: 46926350)
Palbociclib (PubMed CID: 5330286)
Ribociclib (PubMed CID: 44631912)
Riviciclib (PubMed CID: 23643976)
Ronicicliib (PubMed CID: 45380979)
Trilaciclib (PubMed CID: 68029831)
Voruciclib (PubMed CID: 67409219)

Keywords:
Breast cancer
Catalytic spine
K/E/D/D
Protein kinase structure
Protein kinase inhibitor classification
Regulatory spine

ABSTRACT

Cyclins and cyclin-dependent protein kinases (CDKs) are important proteins that are required for the regulation and expression of the large number of components necessary for the passage through the cell cycle. The concentrations of the CDKs are generally constant, but their activities are controlled by the oscillation of the cyclin levels during each cell cycle. Additional CDK family members play significant roles in a wide range of activities including gene transcription, metabolism, and neuronal function. In response to mitogenic stimuli, cells in the G1-phase of the cell cycle produce D type cyclins that activate CDK4/6. These activated enzymes catalyze the monophosphorylation of the retinoblastoma protein. Subsequently, CDK2-cyclin E catalyzes the hyperphosphorylation of Rb that promotes the release and activation of the E2F transcription factor, which in turn lead to the biosynthesis of dozens of proteins required for cell cycle progression. Consequently, cells pass the G1-restriction point and are committed to complete cell division in the absence of mitogenic stimulation. CDK2-cyclin A, CDK1-cyclin A, and CDK1-cyclin B are required for S-, G2-, and M-phase progression. A crucial mechanism in controlling cell cycle progression is the precise timing of more than 32,000 phosphorylation and dephosphorylation reactions catalyzed by a network of protein kinases and phosphoprotein phosphatases as determined by mass spectrometry. Increased cyclin or CDK expression or decreased levels of endogenous CDK modulators/inhibitors such as INK4 or CIP/KIP have been observed in a wide variety of carcinomas, hematological malignancies, and sarcomas. The pathogenesis of neoplasms because of mutations in the CDKs are rare. Owing to their role in cell proliferation, CDKs represent natural targets for anticancer therapies. Palbociclib, ribociclib, and abemaciclib are FDA-approved CDK4/6 inhibitors used in the treatment of breast cancer. These drugs have IC_{50} values for CKD4/6 in the low nanomolar range. These inhibitors bind in the cleft between the N-terminal and C-terminal lobes of the CDKs and they inhibit ATP binding. Like ATP, these agents form hydrogen bonds with hinge residues that connect the small and large lobes of protein kinases. Like the adenine base of ATP, these antagonists interact with catalytic spine residues CS6, CS7, and CS8. These and other CDK antagonists are in clinical trials for the treatment of a wide variety of malignancies. As inhibitors of the cell cycle, it is not surprising that one of their most common toxicities is myelosuppression with decreased neutrophil production.

1. Introduction to the somatic mitotic cell cycle

1.1. An overview of cyclin-dependent protein kinases and their regulatory cyclins

The replication of every cell in every tissue and organ is stringently controlled during development and throughout the life of the individual. In the normal adult, cells replicate only when and where they are needed. Furthermore, each chromosome must be accurately replicated. The cell cycle consists of G1 (Gap1 and presynthetic growth), the S-phase (DNA synthesis), G2 (Gap 2 or premitotic growth), and the M (mitotic) phase (Fig. 1A) [1]. Cells are preparing for DNA synthesis during G1 and they perform surveillance to establish the integrity of newly synthesized DNA during G2 before initiating mitosis. Chromosomal DNA is replicated during the S-phase and the other cellular components are partitioned between two daughter cells during the M-phase. When cells cease proliferating, they exit the cycle and enter a nondividing quiescent state known as G0. Senescence, in contrast, is an

Abbreviations: AS, activation segment; CDK, cyclin-dependent protein kinase; CIP/KIP, CDK interacting protein/kinase inhibitor protein; CS or C-spine, catalytic spine; CL, catalytic loop; ER^+, estrogen receptor positive; GRL, glycine-rich loop; $HER^{+/-}$, human epidermal growth factor receptor positive or negative; HR^+, hormone receptor-positive with either or both estrogen and progesterone receptors; INK4, inhibiting CDK4; NSCLC, non-small cell lung cancer; PKA, protein kinase A; Rb, retinoblastoma protein; RS or R-spine, regulatory spine; Sh1, shell residue 1; WAF1, wild type p53-activated fragment

E-mail address: rrj@brimr.org.

https://doi.org/10.1016/j.phrs.2018.11.035
Received 26 November 2018; Accepted 27 November 2018
Available online 30 November 2018

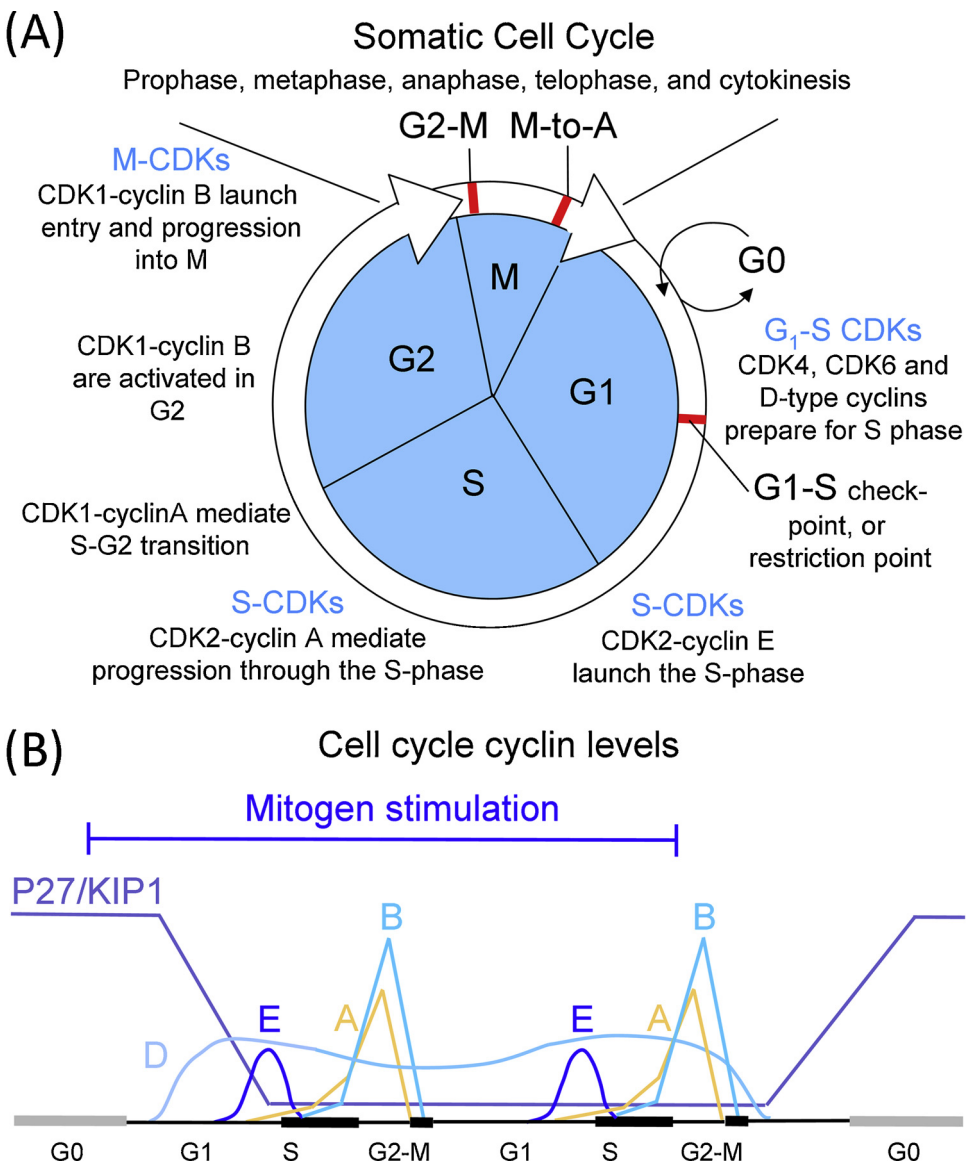

Fig. 1. (A) Overview of the cell division cycle. Adapted from Ref. [2] with copyright permission of Elsevier. (B) Cellular content of cyclins D, E, A, and B in response to mitogenic stimulation; adapted from Ref [3]. with copyright permission of AAAS.

irreversible state of G1 cell cycle arrest in which cells have undergone an irreversible arrest of proliferation and can no longer divide.

Hematopoietic cells or cells that line the intestinal epithelium actively proliferate and cycle continuously [4]. Most other cells in adult animals are generally in a quiescent state or G0-phase, but they can reenter the cell cycle. In contrast, terminally differentiated cells such as cardiac myocytes and neurons have lost the capacity to proliferate and are locked permanently into the G0-phase. Dysregulation of the physiological controls of cellular replication is an underlying defect in cancer. Accordingly, understanding the mechanisms that control cell division is an essential factor in the development of therapeutic modalities for the treatment of cancer. The quandary is to specifically target and deter the growth of cancer cells while not blocking the proliferation of normal cells.

Cyclins and their cognate cyclin-dependent protein kinases (CDKs) are necessary components required for traversing the cell division cycle [5]. Humans possess 20 CDKs (1–20) and 13 cyclin groups (A, B, C, D, E, F, G, H, J, K, L, T, and Y). Fig. 2 depicts the evolutionary relationship of the CDKs, their associated cyclins, and their relative sizes. The CDKs are protein-serine/threonine kinases that belong to the so-called CMGC family (Cyclin-dependent protein kinases, Mitogen-activated protein kinases or MAP kinases, Glycogen synthase kinases, and CDK-like kinases) [7]. Cyclins are activated by a two-step process. CDKs interact with cyclins as a first step in protein kinase activation. Following the formation of the CDK-cyclin complex, the CDK activation segment undergoes phosphorylation at a conserved threonine residue that is catalyzed by CDK7 resulting in the full expression of CDK-cyclin enzyme activity. In most of the literature, the activation segment of CDK is called the T-loop in reference to the conserved threonine. This family of enzymes was initially discovered as proteins that are required for the normal transit through the cell cycle (CDKs 1–6, 11, 14–18) [6]. The CDKs were found later to play important regulatory roles in many diverse functions including the control of gene transcription (CDKs 7–13, 19, 20), epigenetics (CDK1/2/4), metabolism (CDK5/8), neuronal activity (CDK5/16), spermatogenesis (CDK16), and angiogenesis, hematopoiesis, and DNA repair (CDK1/3/9/12) [6,8].

The quantities of the CDKs are more or less constant throughout the cell cycle. The activities of the CDKs that regulate transit through the cell cycle are controlled by the cyclins, proteins whose levels oscillate during the cell cycle [3]. This oscillation of cyclins accounts for their names as they cycle up and down during cell growth and division. CDKs are regulated by a mechanism that involves the biosynthesis (which

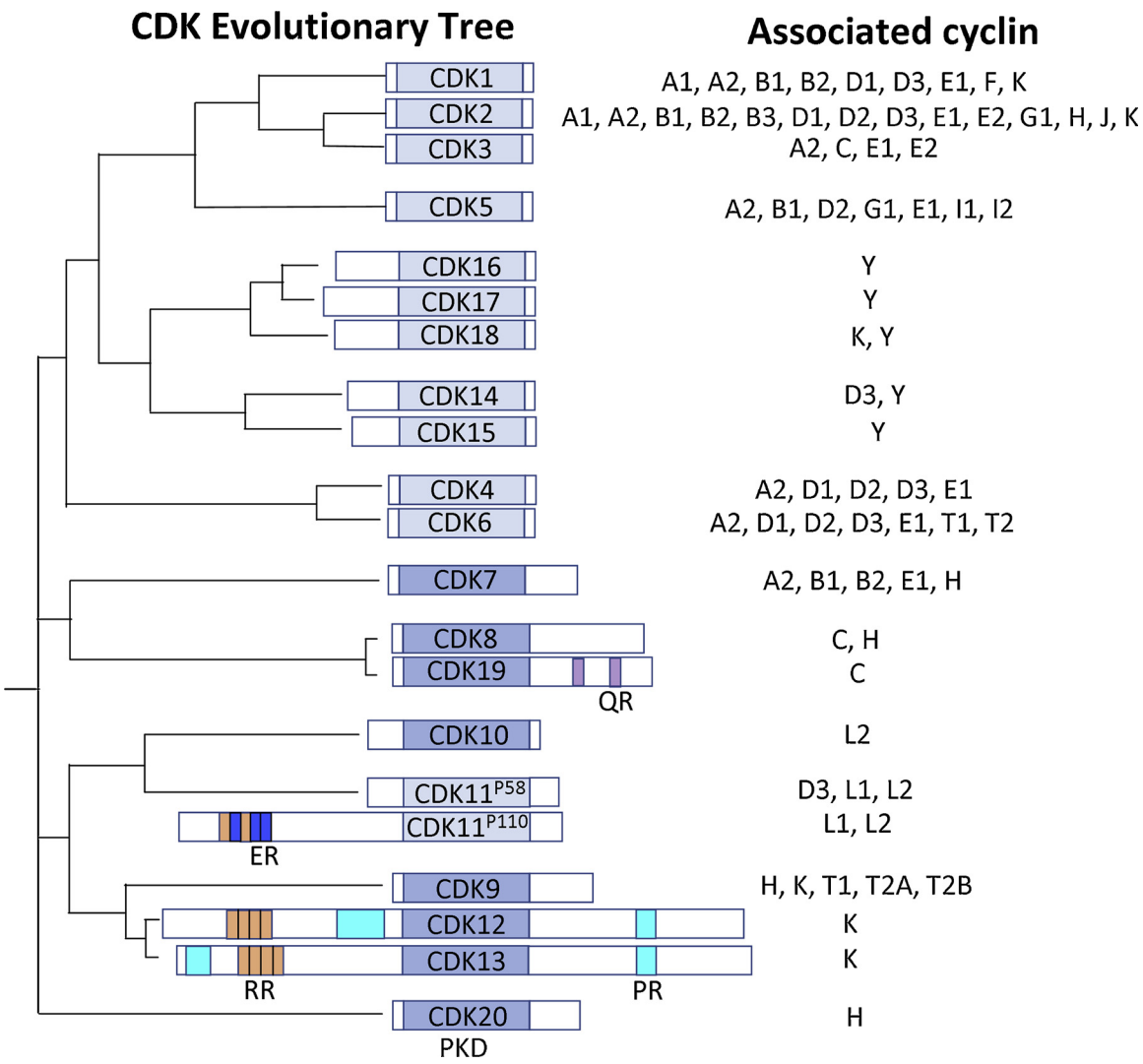

Fig. 2. The evolutionary relationship of the human CDK families. The protein kinase domains (PKD) that are light blue participate in cell cycle regulation and those that are darker blue participate in transcriptional regulation. The cyan colored segments are proline rich (PR), the purple segments are glutamine rich (GR), the orange segments are arginine-serine rich (RR), and the dark blue segments are glutamate rich (ER). Adapted from Ref. [6] with copyright permission of Elsevier.

increases protein kinase activity) and proteolysis (which decreases enzyme activity) of their corresponding cyclins. Most of the CDKs possess about 300 amino acid residues with a molecular weight of about 35 kDa. CDK11 is larger with about 800 amino acid residues and with a molecular weight of about 110 kDa and two of them (CDK12 and CDK13) are much larger with about 1500 residues and a molecular weight of about 165 kDa; the larger proteins contain modular components in addition to the 300 amino-acid–residue protein kinase domain (Fig. 2).

Using human HeLa cells, Arooz et al. found that the peak quantities of cyclin A2 and cyclin E1, at the G2-phase and G1-phase, respectively, were only about 1/8th of that of their partner enzyme (CDK2) [9]. This result indicates that the CDKs are present in excess and are not maximally stimulated by their regulatory subunits. This observation suggests that heightened CDK activity in cancer may be the result of increased cyclin levels rather than increased CDK expression. Experiments to determine the relative amounts of cyclins and their related CDKs in human tumor cells are warranted.

The human cyclins are a large family consisting of about 13 groups of proteins with molecular weights ranging from 35 to 90 kDa [5]. Cyclins are expressed in distinct stages of the cell cycle and are then degraded by an intricately regulated process that involves interactions with ubiquitin ligases (E3s) and proteasomes [10]. This intermittent expression is produced by the cell cycle-dependent activation of the E2F and FOXM1 (forkhead box protein M1) transcription factors [11]. The proteolytic degradation of cyclins is mediated by (i) the Skp1-Cul1-F-box protein (SCF) – which operates from late G1 to early M-phase – and (ii) the anaphase-promoting complex/cyclosome (APC/C) – which acts during anaphase until the end of G1 [12]. The cyclin family consists of three major groups. Group I or the cyclin B group is made up of A, B, D, E, F, G, and J; group II corresponds to cyclin Y; and group III or the cyclin C group is made up of cyclins C, H, K, L, and T (which are major partners with the transcriptional CDKs) [5]. These proteins contain a 100 amino-acid–residue domain consisting of five α-helices called the cyclin box. The A, B, D, E, F, and J cyclins contain two cyclin boxes while the others contain only a single cyclin box.

In order to ensure appropriate advancement through the cell cycle, cells possess a series of checkpoints that block them from progressing into the next phase prematurely or inappropriately before they have successfully finished their current phase. Accordingly, cell-cycle progression can be prevented at these checkpoints when such a transition may be harmful to the cell. The first checkpoint occurs at G1-S (it is also called start, restriction point, or R-point) where G1-S and S-phase CDK-cyclin complexes are activated during G1 (Fig. 1A) [13]. After passing the first checkpoint, completion of the cell cycle is independent of mitogens and growth factors. The G1-S enzymes include CDK4, CDK6,

and the D-type cyclins (D1/2/3), the various forms of which are expressed in a cell and tissue-specific manner. The CDK2-cyclin E complex is required for the transition to the S-phase. G2-M makes up a second checkpoint as the M-phase CDK1-cyclin A/B complex is activated thereby carrying the cell to metaphase during mitosis. The metaphase-to-anaphase transition makes up the third checkpoint, which leads to sister-chromatid segregation, completion of mitosis, and cytokinesis as a single cell completes cell division and forms two daughter cells. Progression results when the M-phase cyclin-CDK complexes stimulate the anaphase-promoting complex, which results in the proteolytic destruction of proteins that hold the sister chromatids together.

Cell cycle progression may be harmful to the cell after DNA undergoes damage by (i) oxidation, alkylation, or hydrolysis of the bases by endogenous processes or (ii) as a result of irradiation or treatment with cytotoxic drugs such as doxorubicin or cisplatin; cell cycle checkpoints are activated following such cellular injuries [14]. Checkpoint activation slows down cell cycle transit and this allows cells to repair the damage before continuing to divide. DNA damage checkpoints occur at the G1/S and G2/M boundaries and within the S-phase. These DNA damage responses involve ATM, ATR, or both protein kinases. These enzymes bind to the chromosomes at the site of DNA damage along with accessory proteins that function as platforms on which DNA damage response elements and DNA repair complexes are assembled. This response occurs as ATM or ATR catalyzes the phosphorylation and consequent activation of Chk1 (checkpoint kinase-1) at S317 and S345; these two residues occur in the carboxyterminal tail downstream from the protein kinase domain. The physiological CDK antagonist p21/CIP/WAF1 is induced by various mechanisms downstream from ATM or ATR and can arrest the cell cycle at checkpoints by inhibiting CDK-cyclin complexes.

Following mitogenic stimulation, one or more cyclin D members – depending upon the cell type – are expressed and promote the activation of CDK4/6, which are crucial regulators of the G1-S transition. The CDK4/6-cyclin D complexes catalyze the phosphorylation of the retinoblastoma (Rb) protein at only one site among 14 potential phosphorylation sites to yield monophosphorylated Rb that exists for several hours in the G1-phase [15]. The biosynthesis of cyclin E activates CDK2 later in the G1-phase thereby leading to (i) the hyperphosphorylation of Rb at all 14 sites and (ii) its deactivation. The CDK2-cyclin E complex mediated Rb hyperphosphorylation is processive in nature; it catalyzes successive reactions without releasing the substrate. The mechanism for promoting cyclin E biosynthesis late in G1 is unclear. (See Ref. [15] for a review of previous notions of Rb phosphorylation and inactivation that include different hypophosphorylated Rb forms). Fully phosphorylated Rb releases its bound E2F transcription factor, which leads to the production of several proteins that are required for cell cycle progression through the G1- and S-phases including Rb itself, cyclin A, and enzymes required for deoxyribonucleotide biosynthesis [16].

CDK4 and CDK6 are protein kinases that exhibit narrow substrate specificity; these enzymes catalyze the phosphorylation of Rb (RB1) and two other Rb-like family proteins (RBL1 or p107 and RBL2 or p130) [1,17]. The generation of cyclin D proteins is followed by the production of cyclin E, cyclin A, and cyclin B along with the activation of their associated CDKs. The relative quantities of cyclin are depicted in Fig. 1B, which is an idealized formulation owing to the differences that occur among various cell types under different conditions. Unlike CDK4 and CDK6, CDK1 and CDK2 exhibit broader specificity and catalyze the phosphorylation of dozens of proteins [1]. The length of the cell cycle varies greatly depending upon the cell type, its location, and the environment; it lasts about a day in rapidly proliferating cells in culture with mitosis lasting about an hour.

Human CDK7 is a subunit of the TFIIH transcription factor; CDK7 participates in the initiation of transcription by catalyzing the phosphorylation of a serine residue within the RNA polymerase II carboxyterminal domain. CDK7 also mediates the phosphorylation and activation of other CDKs, thereby functioning as a CDK-activating kinase (CAK). Unlike the cyclins for cell-cycle–related protein kinases, the cyclins of the transcriptional CDKs fail to exhibit major oscillations in protein concentrations during the cell cycle; rather, their CDK activities are regulated by intricate protein-protein interactions. CDK5 participates in non-cell–cycle related processes including the regulation of insulin secretion, glycogen synthesis, and neuronal functions [8]. CDK14 participates in Wnt/β-catenin signaling and CDK16 plays a role in neuronal function, exocytosis, and spermatogenesis. Like other protein kinases such as ERK1/2, most CDKs are proline-directed protein kinases that catalyze the phosphorylation of a serine or threonine proximal to a proline residue. However, CDK7 can also mediate the phosphorylation of serine or threonine residues in the absence of a targeting proline residue.

1.2. Endogenous CDK polypeptide inhibitors/modulators

In addition to cyclin activation, CDKs are subject to inhibition by two families of endogenous protein inhibitors: CIP/KIP and INK4. These inhibitors can impede cell cycle passage resulting from unfavorable circumstances [18,19]. The CIP/KIP family of three proteins was identified as cell cycle modulators that interact with and inhibit the CDKs. The three family members include p21/CIP/WAF1, p27/KIP1, and p57/KIP2. The maximum concentration of p21/CIP/WAF1 is observed during G1 and G2. The concentration of this protein increases in response to DNA damage by a mechanism that involves the p53 tumor suppressor protein. p27/KIP1 is observed when the cell enters the G0-phase of the cycle and it is degraded following S10 and T187 phosphorylation catalyzed by CDK2; this is followed by E3 ubiquitin ligase-mediated degradation as the cell re-enters G1. p57/KIP2 is a negative regulator of cell proliferation that is expressed in G0 and G1; it inhibits cyclin D-CDK4, cyclin E-CDK2, and cyclin A-CDK2.

The INK4 family of CDK inhibitors has four members: p16/INK4 A, p15/INK4B, p18/INK4C, and p19/INK4D [20]. Each of these antagonists binds to CDK4 and CDK6 and inhibits the binding and activation by the D-type cyclins. Furthermore, each of these CDK antagonists regulates cell cycle G1 progression. p16/INK4 A refers to its molecular weight (in kDa) and its role in inhibiting CDK4 (INK4). p16/INK4 A slows down the transit from the G1 to S-phase when it would be harmful to the cell. Moreover, it acts as a tumor suppressor and is implicated in the prevention of cervical, esophageal, and oropharyngeal squamous cell carcinomas and of melanomas [4]. The p19/INK4D mRNA oscillates in a cell-cycle dependent fashion with the lowest expression at mid G1 and the highest expression during the S-phase. Like p18/INK4C, p19/INK4D plays a role in regulating spermatogenesis [21]. Furthermore, p19/INK4D and p27/KIP1 actively suppress neuronal proliferation of postmitotic brain cells in mice [22].

One feature of the activity of p21/CIP1 and p27/KIP1 is paradoxical [23]. Although these proteins antagonize the activities of CDK2-cyclin E and CDK2-cyclin A, they intensify and stabilize the formation of CDK4/6-cyclin D complexes. Moreover, once a ternary complex including CDK4/6-cyclin D and either p21/CIP1 or p27/KIP2 has formed, the CDK-cyclin–inhibitor ternary complex can still mediate the phosphorylation of its normal substrates. Although p21/CIP1 or p27/KIP1 inhibits the activity of most CDK-cyclin complexes, they fail to inhibit the catalytic activity of CDK4/6-cyclin D. The formation of these ternary complexes operates to remove these inhibitors from CDK2 by the process called CDK inhibitor reshuffling. This progression permits the activation of S-phase CDK activity. Table 1 provides a synopsis of the actions of numerous proteins that participate in the regulation of the somatic mitotic cycle as well as other roles played by the CDKs.

2. Cell cycle dysregulation and cancer

2.1. Cyclins

The unrestrained proliferation of dozens of human cancers is

Table 1
CDKs and other proteins that participate in the regulation of the cell cycle[a].

Cyclin-dependent protein kinases and their cyclin partners		
Enzyme (Uniprot ID)	Major cyclin interactions	Selected CDK functions
CDK1 (P06493)	A1/A2/B1/B2	Triggers S–G2 and G2–M transitions and G2 progression; cyclin A is synthesized in late G1, S, and G2 and is destroyed during prometaphase; B-type cyclins are synthesized in S/G2 and are destroyed following chromosome attachment to the spindle; a major determinant of cell cycle progression
CDK2 (P24941)	E1/E2	Triggers G1–S transition; induces histone biosynthesis and centrosome duplication
	A2	Controls G1–S and G2–M transitions
CDK3 (Q00526)	C	Function is poorly defined [6]; may trigger reentry from G0–G1 and through phosphorylation of Rb; may trigger G1–S transitions by catalyzing the phosphorylation of E2F1/2/3
CDK4/6 (P11802/Q00534)	D1/2/3	Mediates the monophosphorylation of Rb in G1; promotes G1–S transition
CDK5 (Q00535)	D	Function is poorly defined [6]. May produce neuronal cell cycle arrest and differentiation and participates in many aspects of neuronal function
CDK 7 (P50613) or CAK[b]	H	Mediates the activation of CDK1/2/4/6/11 by catalyzing the phosphorylation of a Threonine residue within the T-loop or activation segment; forms part of the TFIIH complex that is important for the regulation of RNA polymerase II transcription and DNA repair; expression and activity are constant during the cell cycle
CDK8 (P49336)	C	Regulation of RNA polymerase II transcription; phosphorylation of NOTCH leads to its degradation
CDK9 (P50750)	T	Regulation of RNA polymerase II transcription
	K	Genome integrity maintenance
CDK10 (Q15131)	M	Traversing start point and phosphorylation of transcription factor ETS2 leading to its degradation
CDK11 A-p110 (Q9UQ88)	L1, L2	Regulation of cell cycle progression, cytokinesis, apoptosis; 8 isoforms
CDK11B (P21127)	L1, L2	Gene duplicate of CDK11 A; regulation of cell cycle progression, cytokinesis, apoptosis; isoform 7 (CDK11-p58) may act as a negative regulator of cell cycle progression
CDK12 (Q9NYV4)	K	Regulation of RNA polymerase II by catalyzing the phosphorylation of its C-terminal tail; regulates genes involved in DNA repair
CDK13 (Q14004)	K	Regulation of transcription elongation and pre-mRNA splicing; required for hematopoiesis
CDK14 (O94921)	D3, Y	Regulator of Wnt signaling during G2 and M; cell cycle progression; neuronal differentiation
CDK15 (Q96Q40)	Y	Antiapoptotic by catalyzing the phosphorylation of BIRC5
CDK16 (Q00536)	Y	Participates in exocytosis, neuron differentiation and development, and spermatogenesis
CDK17 (Q00537)	Y	Functions in terminally differentiated neurons
CDK18 (Q07002)	K, Y	Signal transduction in terminally differentiated cells
CDK19 (Q9BWU1)	C	Positive regulation of apoptosis and inflammation
CDK20 (Q8IZL9)	H	Function is poorly defined [6]; may participate in neural development and the activation of CDK2
Polypeptide inhibitors/modulators of cyclin-dependent protein kinases		
Inhibitor (Uniprot ID)	Targets	Function
p16/INK4 A (P42771)	CDK4/6	Cell cycle arrest in senescence and aging; decreased expression in many cancers
p15/INK4B (P42772)	CDK4/6	Cell cycle arrest in response to transforming growth factor-β; inhibits G2–M transition
p18/INK4C (P42773)	CDK4/6	Cell cycle arrest; inhibits G1–S transition
p19/INK4D (P55273)	CDK4/6	Cell cycle arrest; inhibits G1–S transition
p21/CIP/WAF1 (P38936)	Most CDK-cyclin complexes	Cell cycle arrest after DNA damage; decreased expression in many cancers
p27/KIP1 (P46527)	CDK2/4-cyclin complexes	Cell cycle arrest in G1; both negative and positive effects of cell proliferation owing to CDK4-cyclin D inhibitor shuffling; decreased expression in many cancers
p57/KIP2 (P49918)	CDK2/4-cyclin compleses	Cell cycle arrest in G1; regulation of transcription; decreased expression in many cancers
Other components		
Enzyme (Uniprot ID)	Substrates	Function
Wee1 kinase (P30291)	CDK1 Y15	Nuclear protein kinase; inhibits CDK1-cyclin B in G2 and is a negative regulatory the G2–M transition; levels high in G2 that fall dramatically in M
Myt kinase (Q99640)	CDK1 T14, Y15	Peripheral membrane protein (endoplasmic reticulum and Golgi); inhibits CDK1-cyclinB in G2 and is a negative regulatory of G2–M transition
Cdc25C phosphatase (P30307)	CDK1 pT14, pY15	Promotes G2–M transition; catalyzes the dephosphorylation of CDK1-cyclinA or CDK1-cyclin B at pT14 and pY15

[a] Adapted from Ref. [8].
[b] CAK, CDK-activating protein kinase.

associated with the dysregulation of CDKs [24]. Such dysregulation may involve cyclins, CDKs, or endogenous CDK inhibitors/modulators [2]. As a result, cyclin gene amplification along with protein overexpression, ill-timed cyclin expression, or improper cellular localization can produce inappropriate activation of CDKs [8]. Cyclin D1 amplification occurs in 15–40% of all cancers [25] including melanomas and breast, lung, and oral carcinomas [26]. Schwaederlé et al. found that 50/392 tumor samples bore cyclin D1, D2, D3, and E1 amplifications; these were most commonly associated with breast (22/81 tumor samples), gastrointestinal (10/91), gynecologic (2/33), head and neck (5/39), lung (5/26), melanoma (2/19), nonsolid tumors (2/30), and other neoplasms (2/16); none were observed in 56 brain specimens [27]. Increased cyclin D mRNA levels occur in most multiple myelomas and Bergsagel et al. proposed that dysregulation of cyclin D genes is a unifying oncogenic process in multiple myeloma [28].

Cyclin D1 protein overexpression as determined by immunohistochemical staining has been observed in colorectal, endometrial, head and neck squamous cell, and pancreatic carcinomas as well as NSCLC [2]. The expression of cyclin D activates CDK4 and CDK6 leading to G1-S progression. Cyclin E1 gene amplification was observed in ovarian [29,30] and uterine serous carcinomas [31]. Moreover, cyclin E protein expression is correlated with enhanced malignant behavior of breast, colorectal, ovarian, and pancreatic carcinomas, chronic lymphoblastic leukemias, and a variety of lymphomas [2]. The CDK2-cyclin E complex promotes the transition to the S-phase of the cell cycle (Fig. 1A). Cyclin A protein concentrations are correlated with poorer outcomes in patients with soft tissue sarcomas and endometrial, esophageal, hepatocellular, and thyroid tumors [2]. Cyclin A interacts with CKD2 to facilitate transit through the S-phase and the CDK1-cyclin B complex supports entry into the M-phase of the cell cycle. Moreover, cyclin B concentrations are correlated with poorer outcomes in breast, esophageal, gastric, and non-small cell lung carcinomas.

2.2. Loss of endogenous CDK inhibitors/modulators

The INK4 group of CDK inhibitors acts on CDK4 and 6 to impede

passage through the G1-phase of the cell cycle. The CIP/KIP family can inhibit most CDKs, while still promoting the activity of CDK4/6-cyclin D. p16/INK4 A expression is reduced in acute lymphoblastic leukemias in response to the deletion of its gene [32]. Reduced expression of p16/INK4 A protein has been observed in Hodgkin lymphomas, NSCLC, melanomas, osteosarcomas, and retinoblastomas [2]. In most of these cases, diminished protein expression correlates with poorer patient survival.

Reduced p21/CIP/WAF1 protein expression has been observed in breast, colon, endometrial, and gastric carcinomas and in Hodgkin lymphomas [2]. This is generally correlated with metastases and diminished survival. The highest concentrations of this protein inhibitor occur during progression through G1 and G2. Consequently, p21/CIP/WAF1 decelerates entry into the S- and M-phase of the cell cycle. No or low expression of p27/KIP1 has been reported in breast, colon, esophageal, gastric, and prostate carcinomas as well as pancreatic neuroendocrine tumors. Decreased concentrations are correlated with tumor recurrence and poorer survival. No or low expression of p57/KIP2 protein has been observed in bladder, colorectal, hepatocellular, ovarian, and pancreatic carcinomas. Aberrations in p57/KIP2 expression have also been reported in both adult and childhood acute lymphoblastic leukemias.

2.3. Cyclin-dependent protein kinases

CDK1 protein overexpression has been reported in diffuse large B-cell lymphomas and in melanomas [2]. CDK2/4/8 overexpression occurs in colorectal carcinomas. Additionally, CDK4 gene amplification occurs in cancer of the uterine cervix and in liposarcomas, osteosarcomas, and rhabdomyosarcomas. CDK4 protein overexpression has been reported in melanomas, colorectal carcinomas, NSCLC, and uterine cervical carcinomas. CDK6 gene amplification and overexpression have been observed in gliomas, leukemias, and lymphomas. Moreover, CDK6 is overexpressed in medulloblastomas, which are the most common brain tumors in children, and such overexpression may promote the interaction of the p53 and Rb tumor suppressor pathways [33]. CDK8 is overexpressed in colorectal and gastric carcinomas, CDK9 is overexpressed in pancreatic neuroendocrine tumors and neuroblastomas, CDK11 is overexpressed in osteosarcomas, and CKD14 is overexpressed in esophageal carcinomas [2]. Recall that CDK11 and CDK14 participate in the regulation of the cell cycle while CDK8 and CDK9 are transcription-related enzymes (Table 1).

A large number (71) of different mutations of the CDKs have been described in the catalogue of Cosmic Mutations in Cancer (www.sanger.ac.uk/genetics/CGP/cosmic). However, the incidence of these mutations is very low and only in a few cases, if any, has there been any studies demonstrating that a specific mutation results in increased protein kinase catalytic activity. The low expression of the CDK4 p16/INK4 A inhibitor, the high expression of the CDK4 D-cyclin activator, and the overexpression of CDK4 itself, indicate that CDK4 is a potentially effective drug target for breast, cervical, colorectal, esophageal, hepatic, lung, pancreatic, prostate, and renal carcinomas, NSCLC, acute lymphoblastic lymphomas, mantle cell lymphomas, multiple myeloma, liposarcomas, melanomas, and medulloblastomas [34]. In summary, increases in the expression of the cyclins and CDKs and the decreased expression of CDK inhibitors/modulators occurs in a wide variety of carcinomas, hematological malignancies, and sarcomas. This suggests that a large number of malignancies might be amenable to CDK inhibitor therapy.

2.4. Treatment of breast cancer

The number of newly diagnosed breast cancers in women in the United States and worldwide and the number of deaths is estimated to be 266,000 & 2.08 million and 41,000 & 627,000 in 2018, respectively [35,36]. At the time of the initial diagnosis, about 62% of patients have localized disease, 31% have disease that has just spread to regional lymph nodes, 6% have distant metastases, and 2% have unknown staging (https://seer.cancer.gov/statfacts/html/breast.html). Using statistical models for analyses, the incidence of new female breast cancer cases has been rising about 0.3% each year over the last 10 years. However, the death rates have been decreasing nearly 1.8% each year from 2006 to 2015.

In planning for treatment, breast cancers are grouped into three categories, which are not mutually exclusive. These groups include (i) hormone receptor-positive (HR^+), (ii) overexpression of *ERBB2/HER2/NEU* ($HER2^+$), and (iii) triple-negative breast cancer. Triple-negative breast cancer refers to those lacking (i) estrogen and (ii) progesterone receptors, and (iii) those without *ERBB2/HER2* amplification or overexpression. Wittliff reported that 10–20% of breast cancers are triple-negative and 20–30% overexpress ErbB2/HER2 [37]. He also reported that receptors for estrogen, progesterone, or both occur in about 79% of all breast cancers. Furthermore, he found that 56% of breast cancers contain both the estrogen and progesterone receptors while 14% contain only the estrogen receptor and 9% contain only the progesterone receptor while 21% lack both receptors [37].

Surgery is the principal treatment for localized and advanced breast cancer, followed by radiotherapy, chemotherapy, and adjuvant hormonal therapy (with an aromatase inhibitor or tamoxifen) for HR^+ tumors [2]. Many patients that are HR^+ benefit from treatment with anastrozole or letrozole, which block the formation of the aromatic A ring of estradiol from androgenic precursors. Various cytotoxic drugs are used in the treatment of advanced breast cancers that are HR^- or triple-negative. In patients with $HR^+/HER2^-$ advanced breast cancer that has metastasized, three CDK4/6 antagonists (palbociclib, ribociclib, and abemaciclib) are FDA-approved for their palliative care. Additional drugs that are being considered for the treatment of breast cancer are considered in Section 7.

3. Structures of the cyclin-dependent protein kinases

3.1. Primary structures of the cyclin-dependent protein kinases

The CDKs catalyze the phosphorylation of a protein-serine or threonine residue that occurs immediately before a proline residue. The related ERK/MAP kinases constitute another group of proline-directed kinases [38]. CDK2-cyclin A uses a dual protein substrate recognition mechanism in which the sequence following the phosphoryl acceptor site (S/TPXR/K) is identified by the enzyme *per se* while the cyclin A part of the complex recognizes a downstream R/KXL recruitment motif, where S or T are the phosphorylatable residues and X is any amino acid [39]. CDK2-cyclin E is more discerning than CDK2-cyclin A and these complexes share only a few substrates such as Rb and p27/KIP1 [39]. The CDK1-cyclin B complex uses a similar process for substrate recognition, but it is less stringent about the requirement for the basic amino acid three residues downstream (P + 3) from the phosphorylatable serine/threonine [40]. This bipartite protein-substrate–recognition mechanism of the CDKs differs from that of PKA and most other kinases, which contain a substrate-recognition motif that is entirely within the enzyme [41]. CDK 4 and 6 have narrow substrate specificity while CDK1 and 2 have broad substrate specificity [1]. The chief substrates of CDK4/6 are limited to Rb, p107/RBL1, and p130/RBL2 while the several dozens of substrates of CDK1/2 are necessary for the transit through the S-, G2-, and M-phases of the mitotic cycle [1]. The mechanisms that are responsible for the differences between the broad and narrow substrate specificity of the CDKs are not entirely clear. The stoichiometry of the protein kinase reaction is given by the following chemical equation:

$$MgATP^{1-} + \text{protein–O:H} \rightarrow \text{protein–O:}PO_3^{2-} + MgADP + H^+$$

Hanks and Hunter analyzed the sequences of about 60 protein-

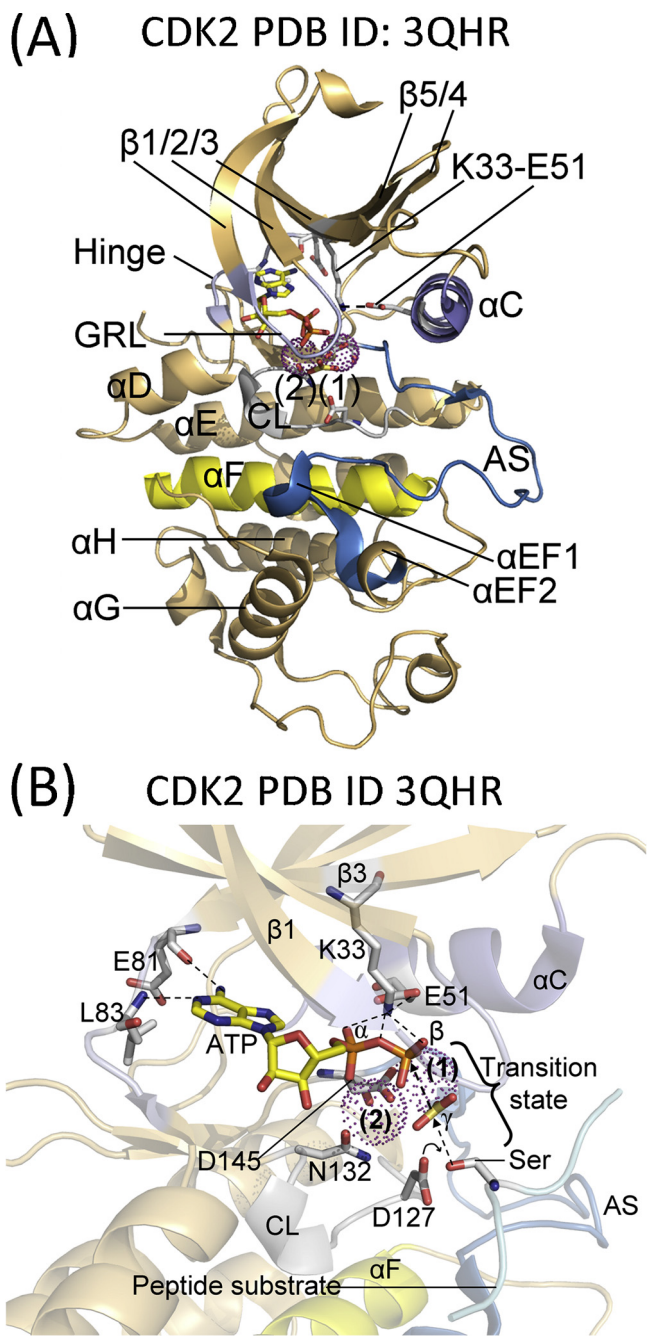

Fig. 3. (A) Overall structure of the active form of the catalytic subunit of CDK2 containing bound ATP, which is located beneath the Gly-rich loop (GRL) and shown in a stick format. The activation segment (AS) is in its active open conformation. (B) Mechanism of the CDK2 reaction of ATP with a peptide substrate with HRD-D127 abstracting a proton from the peptide −OH group. AS, activation segment. Prepared from PDB ID: 1GY3 with the superposition of 3QHR to depict the location of Mg^{2+}(1) and Mg^{2+}(2) (shown as dotted spheres).

serine/threonine and protein-tyrosine kinases and divided the primary structures into 12 domains (I-VIA, VIB-XI) [42]. The protein kinase catalytic domain contains about 300 amino acid residues. Domain I contains a GxGxΦG signature (^{11}GEGTYG^{16} of CDK2), where Φ refers to a hydrophobic residue, and in the case of the CDKs the hydrophobic residue is tyrosine or phenylalanine. The Gly-rich loop (GRL) occurs between the β1- and β2-strands and overlays bound ATP/ADP (Fig. 3A). This is one of the most flexible parts of the enzyme as it accommodates the initial binding of ATP and the subsequent release of ADP. The protein kinase domain II contains a conserved AxK (^{31}ALK^{33}) sequence in the β3-strand and domain III contains a conserved glutamate (E51) residue in the αC-helix that form an electrostatic bond with the conserved AxK-lysine in active protein kinases (K33 and E51 of CDK2). Domain III of CDK1 and 2 contains the sequence PSTAIRE at the beginning of the αC-helix and this sequence interacts with activating cyclins [2]. Domain VIB contains a conserved HRD sequence that forms part of the catalytic loop (^{125}HRDLKPQN^{132} in CDK2). Domain VII contains a ^{145}DFG^{147} signature sequence and domain VIII contains a conserved ^{170}APE^{172} sequence (CDK2) that together signify the beginning and the end of the protein kinase activation segment. The remaining domains make up the αF–αI-helices.

3.2. The K/E/D/D motif and the secondary and tertiary CDK structures

The determination of the X-ray crystallographic structure of PKA provided an invaluable blueprint for understanding the role of the various domains in protein kinase function. Knighton et al. determined the structure of the catalytic subunit of PKA bound to a polypeptide protein kinase antagonist that mimics a peptide substrate (PDB ID: 2CPK) [43,44]. This structure serves as the prototype of all protein kinase catalytic domains including those of the CDK family. CDKs and all protein kinases contain a small amino-terminal lobe and large carboxyterminal lobe [45]. The small N-lobe contains five conserved β-strands and a regulatory αC-helix and the large C-lobe contains eight conserved helices (αD–αI, αEF1, αEF2); the active form of the protein kinase large lobe contains four short strands (β6–β9). The small and large lobes form a cleft that serves as a docking site for ATP. Of the several hundred protein kinase domain structures in the protein data bank, all of them possess this fundamental protein kinase fold as first described for PKA [43–45].

Nearly all active protein kinases possess a conserved K/E/D/D (Lys/Glu/Asp/Asp) signature that plays important structural and catalytic roles [46]. The first two residues are found within the amino-terminal lobe and the second two residues are found within the carboxyterminal lobe. Although both lobes play a part in nucleotide binding, most of the interaction involves the amino-terminal lobe. K33 (the K of K/E/D/D) of the β3-strand of CDK2 binds to the α- and β-phosphates. The carboxylate group of CDK2 E51 (the E of K/E/D/D) of the PSTAIRE αC-helix forms a salt bridge with the ε-amino group of K33 that serves to stabilize its interactions with these phosphates. The presence of an electrostatic bond between the β3-strand lysine and the αC-helix glutamate is a prerequisite for the formation of active protein kinases. This electrostatic bond is significant and is a principal structural topic in the protein kinase literature [46].

The large carboxyterminal lobe participates in nucleotide binding and it makes a major contribution to protein substrate binding. Two Mg^{2+} ions participate in the catalytic cycle of CDK2 [47] and many other protein kinases [48]. CDK2 D145 (the D of DFG and the first D of K/E/D/D) binds to Mg^{2+}(1) (Fig. 3B) that will in turn coordinate the β- and γ-phosphates of ATP. CDK2 N132 of the catalytic loop binds Mg^{2+}(2) that will in turn coordinate with the α- and γ-phosphates of ATP. The γ-phosphate group interacts with a lysine (K129 of CDK2, not shown) within the catalytic loop (^{125}HRDLKPQN^{132}), which is a conserved residue within the protein-serine/threonine kinase family. The β3-strand A31, L83 in the hinge, and L134 after the catalytic loop make hydrophobic contacts with the adenine base of ATP (not shown). Most small molecule protein kinase inhibitors interact with many of the residues within the ATP-binding pocket of this and other protein kinases.

3.3. Structures of the small and large lobes and the protein kinase fold

Like all other protein kinases, the CDK protein kinase domains have a small amino-terminal lobe and large carboxyterminal lobe (Fig. 4A and C). The small lobe contains a conserved flexible glycine-rich ATP-phosphate–binding loop, which is sometimes called the P-loop because

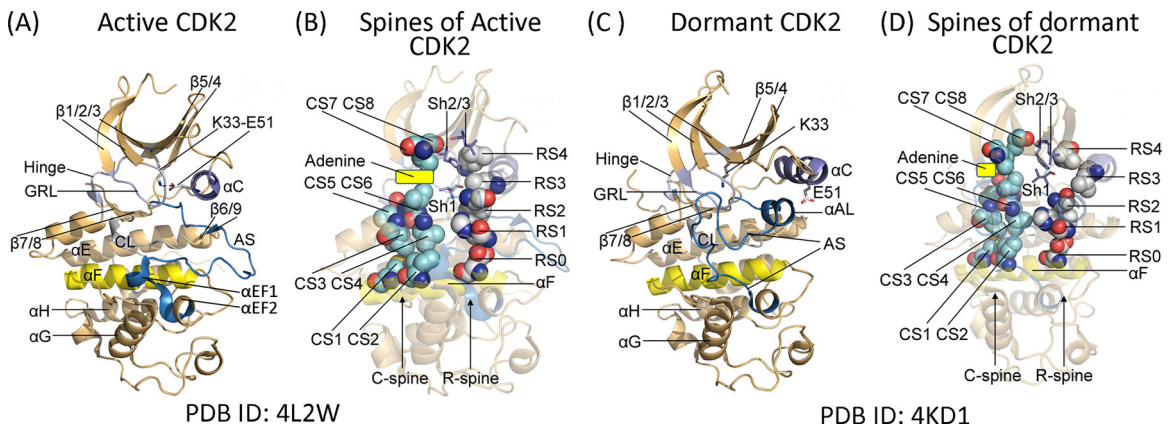

Fig. 4. (A) Diagram of a frontal projection of the classical view of protein kinases depicting the structure of active CDK2. (B) Depiction of the C-spine and R-spine residues of active CDK2 shown as spheres. (C) Inactive CDK2. (D) Spine and shell residues of inactive CDK2. The carbon atoms of the C-spine are sky gray while those of the R-spine are cyan; the shell residues are shown in a stick format with carbon atoms in dark blue. The dashed lines represent a hydrogen bond. AS, activation segment; CL, catalytic loop.

Table 2
Important human CDK2/4/6/9 residues[a].

	CDK2	CDK4	CDK6	CDK9	Inferred function
Protein kinase domain	1–298	6–295	1–326	19–315	Catalyzes substrate phosphorylation
Glycine-rich loop	^{11}GEGTYG^{16}	^{13}GVGAYG^{18}	^{20}GEGAYG^{25}	^{26}GQGTFG^{31}	Anchors ATP β-phosphate
β3-K of K/E/D/D	33	35	43	48	Forms salt bridges with ATP α- and β-phosphates and with αC-E
αC-E, E of K/E/D/D	51	56	61	66	Forms salt bridges with β3-K
Hinge residues	^{81}EFLHQDL^{87}	^{94}EHVDQDL^{100}	^{99}EHVDQDL^{105}	^{104}DFCEHDL^{110}	Connects N- and C-lobes
Catalytic loop	^{125}HRDLKPQN^{132}	^{138}HRDLKPEN^{145}	^{143}HRDLKPQN^{150}	^{147}HRDMKAAN^{154}	Plays both structural and catalytic functions
Catalytic loop HRD-D, First D of K/E/D/D	127	140	145	149	Catalytic base
Catalytic loop HRD(x)$_4$N-N	132	145	150	154	Chelates Mg^{2+}(2)
AS DFG-D, Second D of K/E/D/D	145	158	163	167	Chelates Mg^{2+}(1)
End of AS	^{170}APE^{172}	^{182}APE^{184}	^{187}APE^{189}	^{196}PPE^{198}	Interacts with the αHI loop and stabilizes the AS
AS phosphorylation site	T160	T172	T177	T186	Stabilizes the AS after phosphorylation
No. of amino acids	298	303	326	372	
MW (kDa)	33.9	33.7	36.9	42.8	
UniProtKB accession no.	P24941	P11802	Q00534	P50750	

[a] AS, activation segment.

it is near the phosphates of the ATP substrate. The β3-strand AxK-lysine (CDK2-K33) forms a salt bridge with the conserved glutamate near the center of the protein-kinase αC-helix (CDK2-E51) (Table 2). The formation of a salt bridge between the β3-strand lysine and the αC-helix glutamate is required for the formation of the active enzyme and this structure corresponds to the "αC_{in}" conformation. In contrast, K33 and E51 of dormant CDK2 fail to form a salt bridge and this structure corresponds to the displaced "αC_{out}" conformation (Fig. 4A and C). The αC_{in} conformation is necessary, but not sufficient, for the expression of full protein kinase catalytic activity.

The large lobe contains a mobile activation segment with an extended or open conformation in active enzymes and closed conformation in dormant enzymes. The first residues of the activation segment consist of DFG (Asp-Phe-Gly), which exists in two different conformations. In the dormant activation segment conformation of many protein kinases, the aspartate side chain of the DFG-D sequence extends away from the active site. This is called the "DFG-D_{out}" conformation. The aspartate side chain of active protein kinases extends toward the ATP-binding pocket and coordinates Mg^{2+}(1). This corresponds to the "DFG-D_{in}" conformation. It is the ability of aspartate to bind (DFG-D_{in}) or not bind (DFG-D_{out}) to Mg^{2+}(1) in the active site that is significant. See Ref. [46] for details concerning these two activation segment conformations. However, the inactive conformations of the CDK family exist in the DGF-D_{in} conformation with a closed activation segment, with an αC_{out} conformation, or both.

The C-terminal lobe of the CDK family of protein kinases is mainly α-helical with eight conserved segments (αD–αI, αEF1, αEF2) that occur in all protein kinases [2]. The first X-ray crystallographic structure of PKA possessed two short helices at the end of the activation segment and proximal to the αF-helix, which were unnamed (PDB ID: 2CPK). However, the αEF1/2 helices are conserved in all active protein kinase structures and represent the seventh- and eighth-conserved helices in the C-lobe. The activation segments of protein kinases including the CDK family typically end with APE (Ala-Pro-Glu). The initial portion of the Activation Loop of inactive CDK2 contains an αAL-helix that abuts against the αC-helix that favors an inactive displaced conformation (Fig. 4C). The activation segment of active CDK2 extends outward while that of the less active enzyme is closed and more compact (Fig. 4A and C). The carboxyterminal lobe of active protein kinases contains four short β-strands (β6-β9) (Fig. 4A). The β6-strand, the primary structure of which occurs before the catalytic loop, interacts with the activation segment β9-strand. The primary structure of the β7-strand is located between the catalytic loop and the activation segment and it interacts with the adjacent downstream β8-strand. Most inactive protein kinases including that of CDK2 lack the β6- and β9-strands.

There are two general conformational motions associated with all protein kinases including those of the CDK family. The first involves the interconversion of less active and more active enzyme forms. Activation typically involves changes in the orientation of the αC-helix in the amino-terminal lobe and the activation segment in the carboxyterminal

Table 3
Human CDK2/4/6/9 regulatory spine, shell, and catalytic spine residues.

	Symbol	KLIFS No. Ref. [77]	CDK2	CDK4	CDK6	CDK9
β4-strand (N-lobe)	RS4	38	L66	L74	L79	L81
αC-helix (N-lobe)	RS3	28	L55	L60	L65	L70
Activation loop DFG-F (C-lobe)	RS2	82	F146	F159	F164	F168
Catalytic loop HRD-H (C-lobe)	RS1	68	H125	H138	H143	H147
αF-helix (C-lobe)	RS0	None	D185	D196	D201	D211
Two residues upstream from the gatekeeper	Sh3	43	L78	L91	L96	L101
Gatekeeper, end of the β5-strand	Sh2	45	F80	F93	F98	F103
αC-β4 back loop	Sh1	36	V64	V72	V77	V79
β3-strand AxK-A (N-lobe)	CS8	17	A31	A33	A41	A46
β2-strand V (N-lobe)	CS7	11	V18	V20	V27	V33
β7-strand (C-lobe)	CS6	77	L134	L147	L152	L156
β7-strand (C-lobe)	CS5	76	I135	V148	V153	I157
β7-strand (C-lobe)	CS4	78	L133	I146	L151	V155
αD-helix (C-lobe)	CS3	53	L87	L100	L105	L110
αF-helix (C-lobe)	CS2	None	I192	I203	I208	I218
αF-helix (C-lobe)	CS1	None	M196	M207	M212	M222

lobe. The second class of conformational change occurs as the protein kinase toggles between open and closed conformations as it goes through the catalytic cycle. The open form of the active protein kinase binds MgATP and the protein substrate; this is followed by the formation of the closed form as catalysis occurs. Following catalysis, phosphorylated protein and MgADP are liberated as the enzyme is reconverted to the open form prior to the next catalytic cycle.

CDK2 mediates the in-line nucleophilic attack of the protein-serine/threonine substrate onto the γ-phosphorus atom of Mg_2ATP as first described by Zhou and Adams for PKA (Fig. 3B) [49]. HRD-D127, the catalytic base within the catalytic loop, abstracts a proton from the protein-serine substrate. In such a transition state, the meta-phosphate has dissociated from ADP, but has not yet formed a bond with the protein-seryl group. Mg^{2+}(1) and Mg^{2+}(2) offset the negative charge of the meta-phosphate and the α- and β-phosphates of ATP. In a similar fashion, the positively charged amino group of the β3-strand lysine helps to offset the negative charges of the α- and β-phosphates of ATP.

4. Structure of the CDK hydrophobic skeletons

4.1. The regulatory and catalytic spines

Kornev et al. [50,51] assessed the structures of about two dozen active and inactive protein kinases using a spatial alignment algorithm. They used this information to define a protein kinase (i) regulatory and (ii) catalytic spine. In contrast to protein kinase amino acid signatures such as DFG or HRD, the residues that form the spines were identified by their location as determined by their X-ray crystal structures. The spatial alignment analysis revealed a skeleton of eight hydrophobic residues that constitute a catalytic or C-spine and four hydrophobic residues that make up a regulatory or R-spine.

The R-spine interacts with a conserved aspartate (D185 of CDK2) in the αF-helix. Going from the aspartate within the αF-helix up to the top residue in the β4-strand, Meharena et al. named the regulatory spine residues RS0, RS1, RS2, RS3, and RS4 [52]. As noted later, there are three conserved “shell” residues that interact with the R-spine. We named the catalytic spine residues CS1–CS8 (Fig. 4B and D) [53]. All together each protein kinase contains 16 amino acid residues that make up this protein kinase skeletal composite. Each spine contains residues from both the small and large lobes. The regulatory spine contains residues from the activation segment and the αC-helix, whose spatial arrangements are important in fabricating active and inactive states. The catalytic spine enables ATP binding while the regulatory spine enables the positioning of the protein substrate to promote catalysis. The correct alignment of the spines is required for the formation of an active protein kinase conformation.

The CDK2 regulatory spine consists of a residue from the beginning of the β4-strand (L66, RS4), another that is four residues after the αC-helix E51 (L55, RS3), the phenylalanine of the activation segment DFG-F (F146, RS2), along with the HRD-H (H125, RS1) of the catalytic loop. The backbone of H125 is anchored to the αF-helix by a hydrogen bond to a conserved aspartate residue (D185, RS0). Residues that make up the protein-substrate positioning segment at the end of the activation segment, the αHI-loop, and the catalytic spine of protein kinase domains form hydrophobic contacts with the αF-helix [50]. The αF helix thus serves as a foundation for the key structural elements of protein kinases.

The protein kinase catalytic spine contains residues from the small and large lobes and is completed by the adenine base of ATP [51]. The two residues of the small lobe of CDK2 that bind to the adenine group of ATP include V18 (CS7) near the beginning of the β2-strand and A31 (CS8) from the conserved AxK of the β3-strand. Furthermore, L134 (CS6) from the middle of the carboxyterminal lobe β7-strand contacts the adenine base in the active enzyme. L133 (CS4) and I135 (CS5), hydrophobic residues that flank L134, bind to L87 (CS3) at the beginning of the αD-helix. The αD-helix L87 makes hydrophobic contact with M196 (CS1) in the αF-helix and the β7-strand L133 (CS4) makes hydrophobic contact with I192 (CS2) also in the αF-helix (Fig. 4B and D). Note that both the C-spine and R-spine are anchored to the αF-helix, which is a very hydrophobic component of the enzyme that traverses the entire large lobe.

Table 3 lists the residues of the spines of CDK2/4/6/9. See Refs. [54,55] for a summary of the properties of the ALK receptor protein-tyrosine kinase spine residues, Ref. [2] for the CDK1 spine residues, Ref. [38] for the ERK1/2 protein-serine/threonine kinase spine residues, Ref. [56] for the Janus kinase non-receptor protein-tyrosine kinase spine residues, Ref. [57] for the Kit receptor protein-tyrosine kinase spine residues, Ref. [58] for the MEK1/2 dual-specificity protein kinase spine residues, Ref. [59] for the PDGFRα/β protein-tyrosine kinase spine residues, Refs. [60,61] for the RAF protein-serine/threonine kinase spine residues, Ref. [62] for the RET receptor protein-tyrosine kinase spine residues, Ref. [63] for the ROS1 orphan receptor protein-tyrosine kinase spine residues, Refs. [48] for the Src non-receptor protein-tyrosine kinase spine residues, Ref. [64] for the EGFR/ErbB family of protein-tyrosine kinase spine residues, and Ref. [65] for the VEGFR1/2/3 protein-tyrosine kinase spine residues. The importance of the interaction of therapeutic protein kinase inhibitors with residues that make up the spine residues cannot be overemphasized.

4.2. Shell residues stabilizing the R-spine

Using site-directed mutagenesis methodologies, Meharena et al. discovered three residues in murine PKA that stabilize the R-spine, which they labeled Sh1, Sh2, and Sh3, where Sh refers to shell [52]. The Sh1 V104 G mutant exhibited 5% of the catalytic activity of wild type PKA while the Sh2/Sh3 M120 G/M118 G double mutant was kinase dead. These data indicate that the shell residues support an active protein kinase structure. The Sh1 residue of protein kinases is found in the αC-β4 back loop. The Sh2 or gatekeeper is found at the end of the β5-strand immediately before the hinge, and Sh3 occurs two residues upstream from the gatekeeper in the β5-strand.

Sh1 (V64 of CDK2) interacts with RS3 (L55), Sh2 (F80), and CS6 (L134) while Sh3 (L78) interacts with RS4 (L66) and CS8 (A31) (Fig. 4B and D). Sh2 is the classical gatekeeper residue, which interacts with RS3 (L55), RS4 (L66), and CS7 (V18). The name gatekeeper signifies the role that this residue plays in controlling access to a hydrophobic pocket next to the adenine binding site [66,67] that is occupied by portions of many small molecule antagonists. Based upon the local

spatial pattern alignment data [50], just three of 14 amino acid residues in PKA surrounding RS3 and RS4 are conserved. These shell residues stabilize and reinforce the protein kinase regulatory spine [52]. To reiterate, many therapeutic ATP competitive and allosteric protein kinase inhibitors interact with catalytic spine (CS6/7/8), shell (Sh1), and regulatory spine (RS1/2/3) residues.

5. Classification of protein kinase-drug complexes

Dar and Shokat defined three classes of protein kinase inhibitors and labeled them types I, II, and III [68]. Type I inhibitors bind in the adenine-binding pocket of an active protein kinase; type II inhibitors bind to an inactive protein kinase with the activation segment DFG-D pointing away from the active site (DFG-D_{out}); type III inhibitors bind to an allosteric site that is separate from the adenine-binding pocket. Zuccotto subsequently defined type I½ inhibitors as drugs that bind to an inactive protein kinase with the activation segment DFG-D directed inward (DFG-D_{in}) toward the active site (in contrast to the DFG-D_{out} conformation) [69]. A dormant protein kinase may display a closed activation segment, an αC_{out} conformation, a nonlinear or broken regulatory spine, or various combinations thereof. Gavrin and Saiah then divided allosteric inhibitors into two types: III and IV [70]. Type III inhibitors bind within the cleft between the small and large lobes and next to, but independent of, the ATP binding site while type IV inhibitors bind outside of the cleft. Moreover, Lamba and Gosh described bivalent antagonists as those inhibitors that span two distinct parts of the protein kinase domain as type V inhibitors [71]. For example, a drug that bound to the adenine-binding pocket as well as the peptide substrate site would be classified as a type V inhibitor. To complete this classification, we labeled drugs that bind covalently with the target enzyme as type VI inhibitors [46]. For example, afatinib is a type VI covalent FDA-approved inhibitor of mutant EGFR that is used for the treatment of NSCLC. Mechanistically, this compound binds initially to an active EGFR conformation (like a type I inhibitor) and then the C797 –SH group of EGFR attacks the drug to form an irreversible covalent adduct (PDB ID: 4G5J) [53].

Owing to the variation of inactive protein kinase conformations as compared with the conserved active conformation, it was suggested that type II inhibitors would be more selective than type I inhibitors, which bind to the canonical active conformation. The results of Vijayan et al. support this suggestion [72] while those of Kwarcinski et al. and Zhao et al. do not [73,74]. By definition, type III allosteric inhibitors bind next to the adenine binding pocket [70]. Owing to the greater variability of this region when compared with the adenine-binding site, type III inhibitors have the potential to possess greater selectivity than type I, I½, or II inhibitors. Moreover, Kwarcinski et al. propose that inhibitors that bind to the αC_{out} conformation (type I½ inhibitors) may be more selective than type I and II antagonists [73]. FDA-approved αC_{out} inhibitors include abemaciclib, palbociclib, and ribociclib (all CKD4/6 antagonists). However, Kwarcinski et al. proposed that not all protein kinases are able to assume the αC_{out} conformation while they suggest that all protein kinases are able to adopt the DFG-D_{out} conformation [73].

We divided the type I½ and type II inhibitors into A and B subtypes [53]. Drugs that extend into the back cleft are classified as type A inhibitors. In contrast, drugs that do not extend into the back cleft as are classified as type B inhibitors. Based upon incomplete data, the potential significance of this difference is that type A inhibitors bind to their target enzyme with longer residence times when compared with type B inhibitors [53]. Imatinib is an FDA-approved drug for the treatment of chronic myelogenous leukemia and several other disorders that is a type IIA inhibitor of BCR-Abl that extends far into the back cleft. Bosutinib is an FDA-approved drug for the treatment of chronic myelogenous leukemia that is a type IIB inhibitor of BCL-Abl that does not extend into the back cleft [53].

Ung et al. examined a variety of structural features based upon the location of the DFG-motif and the αC-helix to define the conformational space of the catalytic domain of protein kinases [75]. They reported that the DFG motif can move from its active DFG-D_{in} location to the inactive DFG-D_{out} location. Correspondingly, the αC-helix can move from its active αC_{in} location to the inactive αC_{out} position by rotating and tilting. These authors described five different protein kinase configurations; these include αC_{in}-DFG-D_{in} (CIDI), αC_{out}-DGF-D_{in} (CODI), αC_{in}-DFG-D_{out} (CIDO), αC_{out}-DFG-D_{out} (CODO), and ωCD; the latter designation signifies structures with variable locations of the αC-helix or DFG-D intermediate states. CIDI refers to the catalytically active conformation with a linear R-spine. In contrast, CIDO has the DFG-D motif 180° flip that reshapes the ATP-binding pocket and displaces DFG-F outward thereby breaking the R-spine. CODI signifies the αC_{out} and DFG-D_{in} conformation. This may result from the activation loop displacing the αC-helix to the αC_{out} position. Alternatively, a drug may induce the outward movement of the αC-helix. The CODO conformation is rarely observed. ωCD structures are extremely heterogeneous with diverse DFG-D intermediate states and variable αC-helix positioning. Furthermore, Ung et al. suggest that ωCD structures may represent transition states among the various primary configurations [75].

6. Drug-ligand binding pockets

Liao [76] and van Linden et al. [77] divided the region between the protein kinase small and large lobes into the front cleft or front pocket, the gate area, and the back cleft. The gate area and back cleft make up the back pocket or hydrophobic pocket II (HPII) (Fig. 5). The front cleft includes the hinge residues, the adenine-binding pocket, the glycine-rich P-loop, and the catalytic loop (HRD(x)$_4$N) residues. The gate area includes the β3-strand of the small lobe and the proximal section of the activation segment including DFG of the large lobe. The back-cleft extends to the αC-helix, the αC-β4 back loop, to portions of the β4- and β5-strands of the N-terminal lobe, and to a section of the αE-helix within the C-terminal lobe. One of the obstacles in the development of small molecule protein kinase inhibitors is to increase selectivity to reduce unwanted off-target side effects [78], a process that is aided by examining drug-kinase interactions [79–81].

van Linden et al. described several elements that are found in the front cleft, gate area, and back cleft [77]. For example, the front cleft contains an adenine-binding pocket (AP) along with two front pockets (FP-I and FP-II). FP-I is found between the solvent-exposed hinge residues and the large lobe xDFG-motif (where x is the amino acid immediately before the activation segment DFG) and FP-II is found between the glycine-rich P-loop and the β3-strand at the ceiling of the cleft in the small lobe. BP-I-A and BP-I-B occur in the gate area between the β3- and β4-strands, the conserved β3-strand K of the AxK signature, and the αC-helix of the small lobe and the xDFG-motif of the large lobe. The smaller BP-I-A is found at the top of the gate area and is enclosed by residues of the β3- and adjacent β5-strands including the β3-AxK residues and the regulatory αC-helix. The larger BP-I-B occurs in the center of the gate area allowing for access to the back cleft. Both BP-I-A and BP-I-B are found in both the DFG-D_{in} and DFG-D_{out} conformations (Fig. 5).

BP-II-A-in and BP-II-in occur within the back cleft of the DFG-D_{in} conformation [76]. These sub-pockets are enclosed by the large lobe DFG-motif and the small lobe αC-helix, αC-β4 back loop, and the β4- and β5-strands. Major changes of BP-II-A-in and BP-II-in produce BP-II-out that is found in the DFG-D_{out} configuration; this structural transformation occurs with the movement of DFG-F. The resulting region is called back pocket II-out (BP-II-out); it is found where the DFG-F is located in the DFG-D_{in} configuration. BP-II-B is enclosed by the αC-helix and the adjacent β4-strand in both the DFG-D_{in} and DFG-D_{out} conformations. Back pocket III (BP-III) is observed only in the DFG-D_{out} conformation. This region is found on the floor of BP-II-out between the β6-strand, the conserved catalytic loop HRD-H, the activation segment

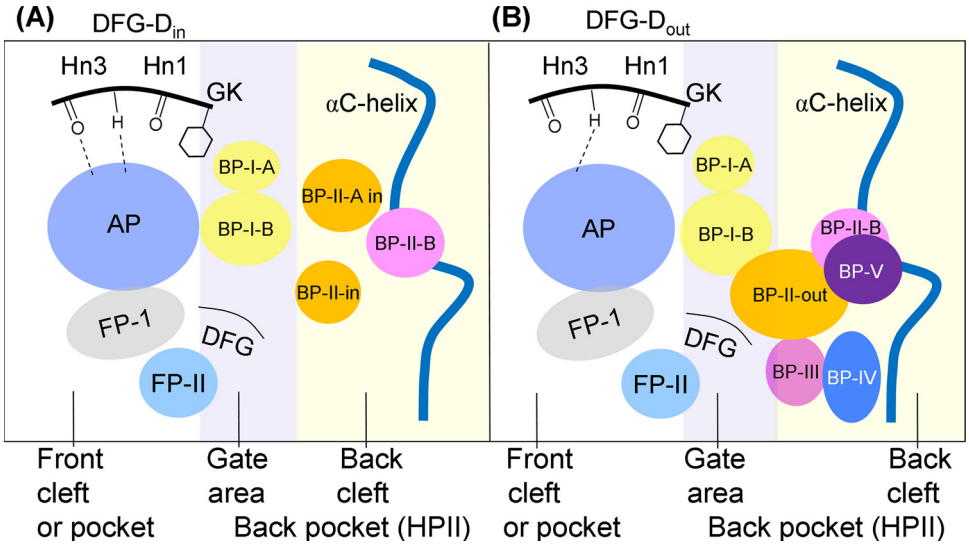

Fig. 5. Location of the protein kinase domain drug-binding pockets. AP, adenine pocket; BP, back pocket; FP, front pocket; Hn, hinge; HPII, hydrophobic pocket II; GK, gatekeeper. Adapted from Ref. [61] with copyright permission of Elsevier.

DFG-D_{out} motif, and the αE-helices of the large lobe along with the αC-β4 back loop and the αC-helix of the small lobe. Two pockets that are partially solvent exposed (BP-IV and BP-V) occur between the small lobe αC-helix and the large lobe DFG-D_{out} motif, the catalytic loop, the β6-strand, and the activation segment (Fig. 5).

van Linden et al. developed a comprehensive guide that describes drug and ligand binding to more than 1200 human and mouse protein kinase domains [77]. Their KLIFS (kinase–ligand interaction fingerprint and structure) directory includes an alignment of 85 potential ligand binding-site residues occurring in both the amino-terminal and carboxyterminal lobes; this directory facilitates the classification of drugs and ligands based upon their binding characteristics and expedites the detection of related interactions. Furthermore, these authors devised a standard amino acid residue numbering system that helps in the comparison of many protein kinases. Table 3 specifies the correspondence between the KLIFS database residue numbers and the catalytic spine, shell, and regulatory spine amino acid residue nomenclature. Furthermore, these investigators established a valuable free and searchable web site that is regularly updated thereby providing comprehensive information on the interaction of protein kinases with drugs and ligands (klifs.vu-compmedchem.nl/). Additionally, Carles et al. developed a comprehensive directory of protein kinase inhibitors in clinical trials [82]. They established a free and searchable web site that is regularly updated which includes inhibitor structures and their physical properties, protein kinase targets, therapeutic indications, year of first approval (if applicable), and trade name (http://www.icoa.fr/pkidb/). The Blue Ridge Insitute for Medical Research website (www.brimr.org/PKI/PKIs.htm), which is regularly updated, depicts the structures and properties of all FDA-approved protein kinase inhibitors.

7. Selected CDK inhibitors that are FDA approved or in clinical trials

Palbociclib is a CDK4/6 antagonist that in combination with the aromatase antagonist letrozole is FDA-approved for (i) the treatment of postmenopausal women with $ER^+/HER2^-$ advanced breast cancer as an initial, or first-line, endocrine-based therapy for metastatic disease or (ii) as a second-line treatment in combination with fulvestrant in women with disease progression following endocrine therapy (www.brimr.org/PKI/PKIs.htm). See Refs. [83–86] for a summary of the preclinical studies and clinical trials that led to these approvals.

The scaffold of palbociclib consists of a pyrido[2,3-*d*] pyrimidinone core (Fig. 6A); this orally effective agent inhibits CDK4-cyclin D1 (IC_{50} value 11 nM), CDK4-cyclin D3 (9 nM), and CDK6-cyclin D2 (15 nM) [87]. It is not effective against CDK2-cyclin E2, CDK2-cyclin A, and CDK1-cyclin B (IC_{50} values exceeding 10 μM). During the development of this compound, VanderWel et al. found that the addition of the cyclopentyl group at *N*8 of the pyrido[2,3-*d*] pyrimidinone core provided an optimal combination of potency and selectivity for CDK4/6 [88]. Moreover, the addition of the *C*5 methyl group decreased CDK1/2 inhibition by these derivatives while they remained effective against CDK4/6. Toogood et al. from the same laboratory discovered that including the 2-aminopyridine on the *C*2 of the scaffold increased selectivity for CDK4/6 *in vitro* [89]. Furthermore, the addition of the acetyl group at *C*6 maintained the selectivity toward CDK4/6.

The X-ray crystal structure of palbociclib bound to the complex of CDK6-cyclin V (a K type cyclin) shows that a hydrogen bond forms between the 2-amino group attached to the pyridopyrimidine scaffold and the carbonyl group of V101 of the hinge of the enzyme (Fig. 7A). Cyclin V is a K-type cyclin that is a gene product of Kaposi sarcoma-associated herpesvirus that activates CDK6. A second hydrogen bond forms between the *N*3 nitrogen of the palbociclib scaffold and the N—H group of V101 while a third hydrogen bond forms between the 6-acetyl carbonyl group and the DFG-D163 N—H group. The 5-methyl and 6-acetyl groups are found within hydrophobic pocket BP—I—A in the gate area [53,77] while the *C*2 piperazinylpyridinylamino group extends into the solvent. Palbociclib makes numerous hydrophobic contacts with the enzyme including interactions with the β1-strand I19, the β2-strand V27 (CS7), the β3-strand A41 (CS8) and K43 (of the AxK signature), V77 (Sh1) within the αC-β4 loop, the F98 gatekeeper (Sh2), the second hinge residue (H100), Q103 and D104 proximal to the αD-helix, Q149 and N150 within the catalytic loop, the β7-strand L152 (CS6), and A162, which occurs just before DFG-D163 of the activation segment (the x of xDFG). The *N*8 cyclopentyl group occupies the space where the ribose of ATP normally occurs. The drug binds to an active conformation of the CDK6-cyclin V complex (αC_{in}, open activation segment, linear R-spine) and is thus a type I inhibitor [53].

The X-ray crystal structure of palbociclib bound to CDK6 without a cyclin (PDB ID: 5L2I) is very similar to that of the CDK6-cyclin V structure (Fig. 7B). However, the drug binds to the αC_{out} conformation of monomeric CDK6 while it binds to the αC_{in} conformation of the CDK6-cyclin V complex. It is likely that the cyclin is responsible for inducing the active-like αC_{in} configuration. The hydrogen bonding pattern is identical as are most of the hydrophobic contacts. Palbociclib makes hydrophobic contacts with the V101 and D102 hinge residues of CDK6, which are lacking in the structure of the CDK6-cyclin V complex.

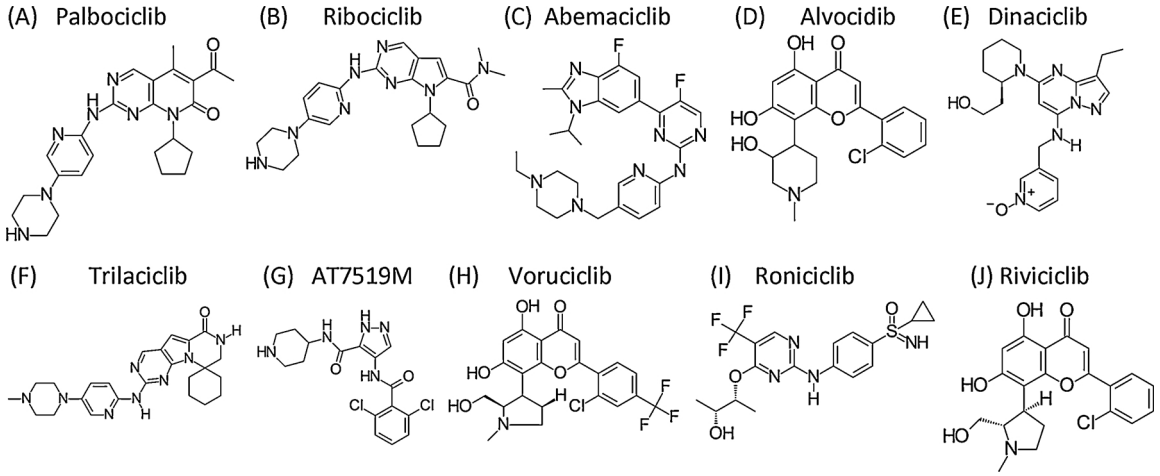

Fig. 6. (A–C) Structures of FDA-approved CDK inhibitors. (D–J) Structures of selected CDK inhibitors in current or previous clinical trials.

The drug binds within the front pocket and does not extend beyond the gate area (making it a type B inhibitor). Because it binds to an inactive enzyme with DFG-D_{in} and αC-helix out, it is classified as a type I½B inhibitor [53]. As noted above, palbociclib is in clinical trials for diseases other than breast cancer and it is possible that its approval for additional clinical indications may be forthcoming as part of various therapeutic regimens.

Ribociclib is an orally effective CDK4/6 inhibitor approved in combination with (i) an aromatase inhibitor for the treatment of pre/perimenopausal or postmenopausal women with HR^+/$HER2^-$ advanced or metastatic breast cancer, as initial endocrine-based therapy or (ii) fulvestrant for the treatment of postmenopausal women with HR^+/$HER2^-$ advanced or metastatic breast cancer, as initial endocrine-based therapy or following disease progression on endocrine therapy (Table 4). See Refs. [90–93] for a summary of the clinical trials that led to these approvals. The core scaffold of ribociclib consists of a pyrrolo [2,3*d*] pyrimidine (Fig. 6B); this drug inhibits CDK4 (IC_{50} value 10 nM) and CDK6 (39 nM) [94]. The inhibitor potency against CDK1 and CDK2 is much less (> 50 μM).

The X-ray crystal structure of ribociclib bound to CDK6 shows that the *N*3 of the pyridine fragment hydrogen bonds with the N—H group of V101 (the third hinge residue) and the adjacent amino group N—H hydrogen bonds with the V101 carbonyl group (Fig. 7C). The drug carbonyl oxygen hydrogen bonds with the N—H group of DFG-D163. Ribociclib makes numerous hydrophobic contacts with the enzyme including interactions with the β1-strand I19, the β2-strand V27 (CS7), the β3-strand A41 (CS8) and K43 (of the AxK signature), V77 (Sh1) within the αC-β4 loop, the F98 gatekeeper (Sh2), the first and second hinge residues (E99, H100), D104 proximal to the αD-helix, T107 of the αD-helix, N150 at the end of the catalytic loop, the β7-strand L152 (CS6), and A162, which occurs just before DFG-D163 of the activation segment (the x of xDFG). Ribociclib is found within the front pocket, the gate area, and FP—I. The drug binds to an inactive conformation of the CDK6 (αC_{out}, DFG-D_{in}, and a nonlinear R-spine) and does not extend beyond the gate area and is thus classified as a type I½B inhibitor [53].

Abemaciclib is an orally effective CDK4/6 inhibitor that is FDA approved (i) in combination with an aromatase inhibitor as initial endocrine-based therapy for the treatment of postmenopausal women with HR^+/$HER2^-$ advanced or metastatic breast cancer (ii) in combination with fulvestrant for the treatment of women with HR^+/$HER2^-$ advanced or metastatic breast cancer with disease progression following endocrine therapy and (iii) as monotherapy for the treatment of

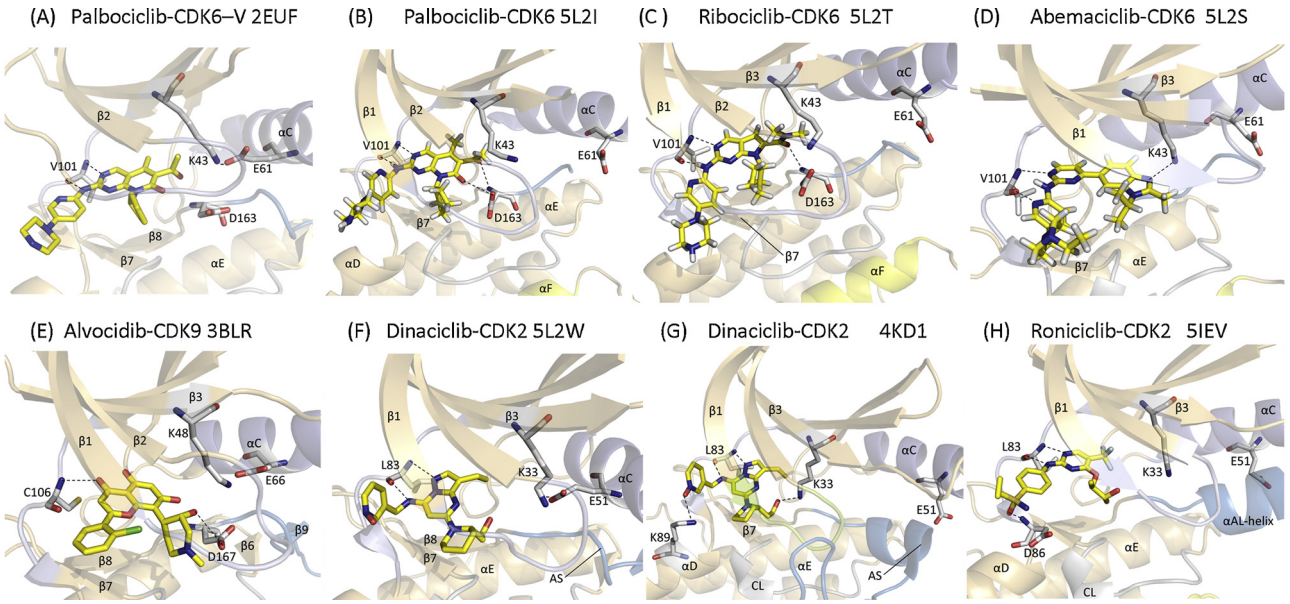

Fig. 7. The protein kinase and corresponding PDB ID of the drug-enzyme complexes are given. The drug carbon atoms are yellow and those of the enzyme are gray. AS, activation segment. The dashed lines represent polar bonds.

Table 4
Selected small molecule CDK inhibitors that have been or are currently in clinical trials.

Drug (code name) trade name	Target	Formula	MW (Da)	D/A[b]	Clinical trial studies[c,d]	No. of Clinical trials[c]
Palbociclib (PD-0332991) Ibrance[a]	CDK4/6	$C_{22}H_{29}N_7O_2$	447	2/8	AML, ALL, breast cancer, bladder cancer, B-cell lymphoma, CRC, Ewing sarcoma, endometrial carcinoma, GIST, HCC, HNSCC, liposarcoma, mantle cell lymphoma, melanoma, non-Hodgkin lymphoma, NSCLC, oligodendroglioma, prostate cancer, pancreatic neuroendocrine tumors, and pancreatic carcinoma	185; 36 completed/terminated, 149 active
Abemaciclib (LY2835219) Verzenio[a]	CDK4/6	$C_{27}H_{32}F_2N_8$	507	1/9	Breast cancer, CRC, endometrial cancer, esophageal cancer, recurrent glioblastoma, HNSCC, lymphoma, mantle cell lymphoma, melanoma, non-Hodgkin lymphoma, NSCLC, pancreatic ductal carcinoma, prostate cancer	59; 11 completed, 48 active
Ribociclib (LEE011) Kisqali[a]	CDK4/6	$C_{23}H_{30}N_8O$	435	2/7	Angiosarcoma, breast, CRC, endometrial carcinoma, glioblastoma, HNSCC, liposarcoma, melanoma, meningioma, myelofibrosis, ovarian carcinoma, NSCLC, pancreatic and prostate cancers	84; 17 completed/terminated, 67 active/recruiting
Alvocidib (L-868275, flavopiridol)	CDK9	$C_{21}H_{20}ClNO_5$	402	2/6	AML, astrocytoma, breast cancer, CLL, endometrial cancer, gastric cancer, GIST, glioma, HNSCC, kidney cancer, liver cancer, lymphoma, melanoma, NSCLC, pancreatic cancer, small cell lung cancer, Waldenström macroglobulinemia	65; 59 completed or terminated, 6 recruiting
Dinaciclib (SCH 727965)	CDK1/2/5/9	$C_{21}H_{28}N_6O_2$	396	2/6	AML, ALL, breast cancer, CLL, mantle cell lymphoma, melanoma, multiple myeloma, pancreatic adenocarcinoma	18; 14 completed or terminated, 4 recruiting;
Trilaciclib (G1T28)	CDK4/6	$C_{24}H_{30}N_8O$	447	2/7	Breast, NSCLC, small cell lung cancer	5; 1 completed, 4 active
(SHR6390)	CDK4/6	Unknown			Breast, CRC, gastric carcinoma, liver cancer, NSCLC	5; 3 planned, 2 unknown status
(AT7519)	CDK1/2/4/6/9	$C_{16}H_{17}Cl_2N_5O_2$	382	4/4	CLL, lymphoma, mantle cell lymphoma, multiple myeloma	5; 4 completed, 1 recruiting
Voruciclib (P1446 A-05)	CDK9	$C_{22}H_{19}ClF_3NO_5$	470	3/9	CLL, melanoma	5; 4 completed or suspended, 1 recruiting
Roniciclib (BAY 1000394)	CDK1/2/3/4/7/9	$C_{18}H_{21}F_3N_4O_3S$	430	3/10	NSCLC, small cell lung carcinoma, thyroid cancer	9; all completed or terminated
Riviciclib (P276-00)	CDK1/4/9	$C_{21}H_{20}ClNO_5$	402	3/6	Breast, HNSCC, mantle cell lymphoma, melanoma, multiple myeloma, pancreatic carcinoma	11; all completed or terminated

[a] FDA approved for the treatment of breast cancer.
[b] D/A; No. of H-bond Donors/Acceptors.
[c] From clinicaltrials.gov accessed 26 November 2018.
[d] ALL, acute lymphoblastic leukemia; AML, acute myeloblastic leukemia; CLL, chronic lymphoblastic leukemia; CRC, colorectal cancer; GIST, gastrointestinal stromal tumor; HCC, hepatocellular carcinoma; HNCC, head and neck squamous cell carcinoma; NSCLC, non-small cell lung cancer.

Table 5
Drug-CDK2/6/9 hydrophobic (Φ), hydrogen bonding (H), and polar (P) interactions based upon their KLIFS residue numbers[a,b].

KLIFS No. Ref. [77]	Location	Palbociclib-CDK6-cycin E, 2EUF[c]	Palbociclib-CDK6, 5L2I[c]	Ribociclib-CDK6, 5L2T[c]	Abemaciclib-CDK6, 5L2S[c]	Alvocidib-CDK9-cyclin T1, 3BLR[c]	Dinaciclib-CDK2-cyclin E, 5L2W[c]	Dinaciclib-CDK2, 4KD1[c]	Roniciclib-CDK2, 5IEV[c]
1	Dom I, Front Cleft								
2	Dom I, Front Cleft								
3	Dom I, Front Cleft	Φ	Φ	Φ	Φ	Φ	Φ	Φ	Φ
4	GRL, Front Cleft	Φ		Φ	Φ	Φ	Φ	Φ	Φ
5	GRL, Front Cleft						Φ	Φ	
6	GRL, Front Cleft	Φ					Φ	Φ	
7	GRL, Front Cleft								
8	GRL, Front Cleft				Φ	Φ			
9	GRL, Front Cleft								
10	Dom II, Front Cleft								
11	Dom II, Front Cleft	Φ	Φ	Φ	Φ	Φ	Φ	Φ	Φ
15	β3-K	Φ	Φ	Φ	Φ, P	Φ	Φ	Φ, P	Φ
16	Dom II, Gate Area								
17	Dom III, Gate Area	Φ	Φ	Φ	Φ	Φ		Φ	
36	αC-β4, Back Loop	Φ	Φ	Φ	Φ	Φ	Φ	Φ	Φ
45	Gatekeeper	Φ	Φ	Φ	Φ	Φ		Φ	Φ
46	Hinge, Front Cleft			Φ	Φ		Φ	Φ	
47	Hinge, Front Cleft	Φ	Φ	Φ	Φ	Φ	Φ	Φ	Φ
48	Hinge, Front Cleft	H, Φ	H	H	H, Φ	H, Φ	H, Φ	H, Φ	H, Φ
49	Hinge, Front Cleft	Φ			Φ	Φ	Φ	Φ	Φ
51	Hinge, Front Cleft	Φ	Φ		Φ	Φ	Φ	Φ	Φ
52	Hinge, Front Cleft	Φ	Φ	Φ	Φ	Φ		Φ	Φ
55	αD-helix, Front Cleft	Φ		Φ	Φ			Φ	Φ
68	CL-H, Front Cleft								
69	CL-R, Front Cleft								
70	CL-D, Front Cleft								
74	CL, Front Cleft	Φ	Φ		Φ	Φ	Φ	Φ	Φ
75	CL-N, Front Cleft	Φ	Φ	Φ		Φ	Φ	Φ	Φ
76	Dom VII, Front Cleft								
77	Dom VII, Front Cleft	Φ	Φ	Φ	Φ	Φ	Φ	Φ	Φ
80	x, Gate Area	Φ	Φ	Φ	Φ	Φ	Φ	Φ	Φ
81	AS-D, Gate Area	Φ	Φ, P	Φ, P	Φ	Φ, P	Φ		Φ
82	AS-F, Gate Area								
83	AS-G, Gate Area								

[a] AS, activation segment; CL, catalytic loop; Dom, Hanks domain [42]; GRL, glycine-rich loop; x, residue immediately before DFG.
[b] klifs.vu-compmedchem.nl/.
[c] Protein data base ID.

patients with $HR^+/HER2^-$ advanced or metastatic breast cancer with disease progression following endocrine therapy and prior chemotherapy in the metastatic setting. The latter indication is the only CDK inhibitor monotherapy approval. See Refs. [95–98] for a summary of the clinical trials that led to these approvals. The scaffold of abemaciclib consists of a pyridine-pyrimidine-benzimidazole core (Fig. 6C) [99].

The X-ray crystal structure of abemaciclib bound to CDK6 shows that the *N*1 of the pyrimidine fragment hydrogen bonds with the N−H group of V101 (the third hinge residue) and the adjacent amino group N−H hydrogen bonds with the V101 carbonyl group (Fig. 7D). The *N*1 of the benzimidazole of the drug hydrogen bonds with the ε-amino group of the β3-strand K43. Abemaciclib makes numerous hydrophobic contacts with the enzyme including interactions with the β1-strand I19, the β2-strand V27 (CS7), the β3-strand A41 (CS8) and K43 (of the AxK signature), V77 (Sh1) within the αC-β4 loop, the F98 gatekeeper (Sh2), the first and second hinge residues (E99, H100), D104 proximal to the αD-helix, T107 of the αD-helix, the β7-strand L152 (CS6), and A162, which occurs just before DFG-D163 of the activation segment (the x of xDFG). Abemaciclib is found within the front pocket and FP−II. The drug binds to an inactive conformation of the CDK6 (αC_{out}, DFG-D_{in}, and a nonlinear R-spine) and does not extend beyond the gate area and is thus classified as a type I½B inhibitor [53].

Alvocidib (flavopiridol) is a piperidine-chromenone derivative (Fig. 6D) that is not FDA approved, but is in clinical trials for breast, endometrial, and several other cancers and hematological malignancies (Table 4) [100–104]. This drug targets CDK9 (IC_{50} = 3.2 nM) and CDK4 (IC_{50} = 3.2 nM), it also inhibits other CDKs (CDK1/2/3/6/7), but with IC_{50} values that are 1–2 orders of magnitude higher. The X-ray crystal structure of alvocidib bound to CDK9 shows that the *C*4 carbonyl group of the chromenone forms a hydrogen bond with the third hinge residue (C106) and the 3-hydroxyl group on the piperidine ring hydrogen bonds with DFG-D167 (Fig. 7E). The drug makes hydrophobic contact with the enzyme including interactions with the β1-strand I25, F30 within the G-rich loop, the β2-strand V33 (CS7), the β3-strand A46 (CS8) and K48 (of the AxK signature), V79 (Sh1) within the αC-β4 loop, the F103 gatekeeper (Sh2), the hinge residues F105, E107, H108, as well as A153 and N154 within the catalytic loop, the β7-strand L156 (CS6), and A166, which occurs just before DFG-D167 of the activation segment (the x of xDFG), and DFG-D167. The drug binds to an active conformation of the CDK9 (αC_{in}, open activation segment, linear R-spine) and is thus a type I inhibitor [53].

Dinaciclib is a pyrazolopyrimidine derivative (Fig. 6E) that is not FDA approved, but is in clinical trials for the treatment of breast and pancreatic cancer and several leukemias (Table 4) [105–111]. This drug targets CDK1/2/5/9 with IC_{50} values of 3.2, 1, 1, and 4 nM, respectively. The X-ray crystal structure of the drug bound to the CDK2-cyclin E complex shows that the pyrazolo nitrogen forms a hydrogen bond with the N−H group of L83 (the third hinge residue) and the amino group of the drug forms a hydrogen bond with the L83 carbonyl group (Fig. 7F). The drug makes hydrophobic contact with the enzyme including interactions with the β1-strand I10, the β2-strand V18 (CS7), the β3-strand A31, V64 (Sh1) within the αC-β4 loop, the F80 gatekeeper (Sh2), the hinge residues E81, F82, L83, H84, and Q85, Q131 and N132 within the catalytic loop, the β7-strand L134 (CS6), A144, which occurs just before DFG-D145 of the activation segment (the x of xDFG), and DFG-D145. The drug binds to an active conformation of the CDK2-cyclin E complex (αC_{in}, open activation segment, linear R-spine) and is thus a type I inhibitor [53]. The X-ray crystal structure of dinaciclib bound to CDK2 is very similar in terms of hydrogen bonding and hydrophobic interactions. However, the enzyme is in an inactive αC_{out} conformation (Fig. 7G) and consequently the mode of inhibitor binding corresponds to a type I½B inhibitor [53]. Moreover, both structures show that dinaciclib binds within the front pocket and does not extend to the gate area.

Roniciclib is an anilino-pyrimidine CDK multikinase inhibitor (Fig. 6I) [112,113] that has been in clinical trials for the treatment of ovarian cancer, small cell lung cancer, and thyroid cancer (Table 4) [114]. The X-ray crystal structure shows that the *N*1 of the pyrimidine ring hydrogen bonds with the N−H group of L83 and the amino group of the drug hydrogen bonds with the carbonyl group of L83, the third hinge residue (Fig. 7H). The sulfonimidoyl oxygen forms a hydrogen bond with the N−H group of D86 within the hinge. The drug makes numerous hydrophobic contacts with the enzyme including interactions with the β1-strand I10, the β2-strand V18 (CS7), the β3-strand A31 (CS8), V64 (Sh1) of the back loop, the F80 gatekeeper residue, F82, H84, Q85, D86 of the hinge, the αD-helix K89, the catalytic loop Q131 and N132, A144 (the x residue of xDFG), and DFG-D145. The drug binds to the front pocket and FP−I of CDK2. It binds to an inactive αC_{out}/DFG-D_{in} (CODI) conformation is therefore classified as a type I½B inhibitor [53]. It is unclear whether the drug will progress any further in clinical trials.

A summary of the drug-CDK2/6/9 hydrophobic (Φ), hydrogen-bonding (H), and polar-bonding (P) interactions based upon the KLIFS residue numbers is provided in Table 5. The KLIFS system gives comparable residues from different enzymes the same value [77], which facilitates comparisons among different protein kinases. The various Hanks domains correspond to those that are listed in Ref. [42]. All of the drugs interact hydrophobically with the Hanks/KLIFS domain I/residue 3, domain II/residues 11 and 15, the back-loop residue 36, domain VII/residue 77, and the x residue immediately before DFG. Residue 3 occurs immediately before the G-rich loop, residue 11 corresponds to CS7 and residue 15 corresponds to CS8, residue 36 corresponds to the conserved valine in the αC-β4 back loop (Sh1), and residue 77 corresponds to CS6 (Table 3). All of the drugs form hydrogen bonds with the third hinge residue. Most of the drugs make hydrophobic contact with (i) the first residue in the G-rich segment, (ii) the side chain of the AxK-lysine, (iii) the gatekeeper phenylalanine, (iv), the penultimate residue as well as the last residue in the catalytic loop, and (v), the DGF-D side chain. The drugs make variable hydrophobic interactions with KLIFS residues 5, 6, and 8 within the G-rich loop, with hinge residues 46 (the first hinge residue), 49 (the forth hinge residue), 51 (the sixth hinge residue), and 52 (the seventh hinge residue). Palbociclib, ribociclib, and alvocidib make polar bonds with DFG-D and abemaciclib and dinaciclib make polar contact with the β3-strand lysine residue.

Trilaciclib [115–117], AT7519 [118–121], and voruciclib [122–124] are CDK inhibitors (Fig. 6F–H) that are currently in clinical trials for the treatment of a variety of diseases (Table 4). The structure of SHR6390 [125], which is also in clinical trials, is unknown. Riviciclib is a CDK1/4/9 inhibitor (Fig. 6J) that has been in clinical trials, but in the absence of any new data it is unlikely that his drug will be approved [2]. Unfortunately, we lack X-ray crystal structures of these compounds bound to any protein kinase. All of the drugs listed in Table 4 are orally effective – with the exception of alvocidib and riviciclib, which are given intravenously. See Ref. [6] for the listing of other CDK inhibitors that are or have been in clinical trials, but are no longer considered promising therapeutic agents.

8. Epilogue

The progression through the cell cycle is an intricate process that involves the precise timing of more than 32,000 phosphorylation and dephosphorylation reactions catalyzed by a network of protein kinases and phosphoprotein phosphatases as determined by mass spectrometry [126]. The mechanism of cell cycle progression has been studied for about 45 years [127]. In a pioneering study, Hartwell et al. used a genetic approach and characterized several cell division cycle (CDC) temperature-sensitive mutants of *Saccharomyces cerevisiae* whose gene function was required at specific stages of the cell cycle [128]. His initial collection of cell cycle mutants contained changes in what we now recognize as key regulators of the eukaryotic cell cycle. These include

CDC28 (CDK1), *CDC4* (cell division control protein-4) that facilitates ubiquitylation and thereby destruction of CDK inhibitory proteins (SIC1, CDC6) and is required at G1-S and G2-M transitions as well as components of the anaphase promoting complex or cyclosome (APC/C) involved in promoting cyclin degradation [127]. Nurse similarly used a genetic approach and isolated temperature-sensitive mutants of *Schizosaccharomyces pombe* that produced smaller size cells than those that divided at the permissive temperature [129]. These *wee-1* or small mutants encoded a protein kinase (Wee-1) that catalyzed the phosphorylation and inhibition of CDK1 (Table 1) [127].

Evans and Hunt et al. used a biochemical approach and investigated the regulation of mRNA translation in embryos of the sea urchin *Arbacia punctulata* [130]. Protein synthesis in young dividing embryos is encoded by stored maternal mRNAs, which correspond to a few abundant proteins whose synthesis is barely, if at all, detectable in the unfertilized egg. One of these proteins, which was named cyclin, was degraded every time that the cells divide. After fertilization, cyclin robustly incorporated [^{35}S]- methionine only to be broken down after mitosis. Moreover, the protein was again labeled during the next cycle only to be degraded yet again at the end of the cycle.

Many investigators participated in the studies on the regulation of the cell cycle and experiments indicated that the process was conserved across many eukaryotic species including humans [127]. Because cancer cells exhibit dysregulated cell division along with the presence of abnormal chromosome numbers (aneuploidy) [131], it was natural to focus on cell cycle inhibitors as potential anticancer agents [132]. Among the first studies addressing the potential of CDK antagonists as anticancer agents was that by Kaur et al. in 1992 who investigated the effects of alvocidib (flavopiridol) on several breast and lung cancer cell lines [133]. It was not until 2015 that palbociclib in combination with letrozole was approved by the FDA as a first-line treatment for HR$^+$/HER2$^-$ breast cancer (www.brimr.org/PKI/PKIs.htm). The FDA subsequently approved the combination of palbociclib and fulvestrant as a second-line therapy in women with disease progression following endocrine therapy. The development of a clinically approved CDK4/6 inhibitors required about two dozen years, which contrasts with the time-line for the development of an ALK antagonist (crizotinib) over four years or EGFR inhibitors (erlotinib and gefitinib) over nine years [54]. As noted in Table 4, abemaciclib, palbociclib, ribociclib, and other CDK antagonists are undergoing clinical trails for a variety of cancers as a single agent or as part of a combination of drugs.

One of the main difficulties in cancer therapy is the development of resistance to both targeted and nontargeted drugs. Owing to the recent introduction of CDK inhibitors into the clinic, only lately have there been studies addressing mechanisms of resistance to these agents [134,135]. Preclinical studies suggest that secondary or acquired resistance may be mediated by AKT/PKB and mTOR signaling pathway that remains active in the presence of CDK4/6 inhibitors [136]. Preclinical studies performed by Yang et al. suggest that *CDK6* gene amplification and decreased expression of the estrogen and progesterone receptors may contribute to resistance [137]. Moreover, these investigators observed reduced hormone receptor expression in tumor samples taken from patients who had developed resistance to abemaciclib or ribociclib. One strategy for minimizing the development of resistance is the use of combination therapies. The use of palbociclib or ribociclib in combination with exemestane (an aromatase inhibitor) and everolimus (an mTOR inhibitor that is FDA-approved for the treatment of HER2$^-$ breast cancer) represents one strategy for mitigating drug resistance by targeting multiple signaling pathways [138]. Devising protocols for minimizing or overcoming resistance to cancer therapies constitutes one of the most important problems faced by biomedical scientists and oncologists who work on anticancer therapies.

Conflict of interest

The author is unaware of any affiliations, memberships, or financial holdings that might be perceived as affecting the objectivity of this review.

Acknowledgments

The colored figures in this paper were evaluated to ensure that their perception was accurately conveyed to colorblind readers [139]. The author thanks Laura M. Roskoski for providing editorial and bibliographic assistance. I also thank Josie Rudnicki and Jasper Martinsek for their aid in preparing the figures and Pasha Brezina and W.S. Sheppard for their help in structural analyses.

References

[1] M. Malumbres, M. Barbacid, Mammalian cyclin-dependent kinases, Trends Biochem. Sci. 30 (2005) 630–641.
[2] R. Roskoski Jr., Cyclin-dependent protein kinase inhibitors including palbociclib as anticancer drugs, Pharmacol. Res. 111 (2016) 784–803.
[3] C.J. Sherr, Cancer cell cycles, Science 274 (1996) 1672–1677.
[4] M. Malumbres, M. Barbacid, To cycle or not to cycle: a critical decision in cancer, Nat. Rev. Cancer 1 (2001) 222–231.
[5] M. Malumbres, Cyclin-dependent kinases, Genome Biol. 15 (2014) 122.
[6] S.R. Whittaker, A. Mallinger, P. Workman, P.A. Clarke, Inhibitors of cyclin-dependent kinases as cancer therapeutics, Pharmacol. Ther. 173 (2017) 83–105.
[7] G. Manning, D.B. Whyte, R. Martinez, T. Hunter, S. Sudarsanam, The protein kinase complement of the human genome, Science 298 (2002) 1912–1934.
[8] M. Peyressatre, C. Prével, M. Pellerano, M.C. Morris, Targeting cyclin-dependent kinases in human cancers: from small molecules to peptide inhibitors, Cancers (Basel) 7 (2015) 179–237.
[9] T. Arooz, C.H. Yam, W.Y. Siu, A. Lau, K.K. Li, R.Y. Poon, On the concentrations of cyclins and cyclin-dependent kinases in extracts of cultured human cells, Biochemistry 39 (2000) 9494–9501.
[10] K.I. Nakayama, K. Nakayama, Ubiquitin ligases: cell-cycle control and cancer, Nat. Rev. Cancer 6 (2006) 369–381.
[11] S. Lim, P. Kaldis, Cdks, cyclins and CKIs: roles beyond cell cycle regulation, Development 140 (2013) 3079–3093.
[12] F. Bassermann, R. Eichner, M. Pagano, The ubiquitin proteasome system - implications for cell cycle control and the targeted treatment of cancer, Biochim. Biophys. Acta 1843 (2014) 150–162.
[13] W. Kolch, M. Halasz, M. Granovskaya, B.N. Kholodenko, The dynamic control of signal transduction networks in cancer cells, Nat. Rev. Cancer 15 (2015) 515–527.
[14] M. Goldstein, M.B. Kastan, The DNA damage response: implications for tumor responses to radiation and chemotherapy, Annu. Rev. Med. 66 (2015) 129–143.
[15] A.M. Narasimha, M. Kaulich, G.S. Shapiro, Y.J. Choi, P. Sicinski, S.F. Dowdy, Cyclin D activates the Rb tumor suppressor by mono-phosphorylation, Elife 3 (2014).
[16] J.M. Trimarchi, J.A. Lees, Sibling rivalry in the E2F family, Nat. Rev. Mol. Cell Biol. 3 (2002) 11–20.
[17] L. Anders, N. Ke, P. Hydbring, Y.J. Choi, H.R. Widlund, J.M. Chick, et al., A systematic screen for CDK4/6 substrates links FOXM1 phosphorylation to senescence suppression in cancer cells, Cancer Cell 15 (20) (2011) 620–634.
[18] N.G. Starostina, E.T. Kipreos, Multiple degradation pathways regulate versatile CIP/KIP CDK inhibitors, Trends Cell Biol. 22 (2012) 33–41.
[19] K.M. LaPak, C.E. Burd, The molecular balancing act of p16(INK4a) in cancer and aging, Mol. Cancer Res. 12 (2014) 167–183.
[20] E.T. Cánepa, M.E. Scassa, J.M. Ceruti, M.C. Marazita, A.L. Carcagno, P.F. Sirkin, et al., INK4 proteins, a family of mammalian CDK inhibitors with novel biological functions, IUBMB Life 59 (2007) 419–426.
[21] F. Zindy, W. den Besten, B. Chen, J.E. Rehg, E. Latres, M. Barbacid, et al., Control of spermatogenesis in mice by the cyclin D-dependent kinase inhibitors p18(Ink4c) and p19(Ink4d), Mol. Cell. Biol. 21 (2001) 3244–3255.
[22] F. Zindy, J.J. Cunningham, C.J. Sherr, S. Jogal, R.J. Smeyne, M.F. Roussel, Postnatal neuronal proliferation in mice lacking Ink4d and Kip1 inhibitors of cyclin-dependent kinases, Proc. Natl. Acad. Sci. U. S. A. 96 (1999) 13462–13467.
[23] J. Cicenas, K. Kalyan, A. Sorokinas, A. Jatulyte, D. Valiunas, A. Kaupinis, et al., Highlights of the latest advances in research on CDK inhibitors, Cancers (Basel) 6 (2014) 2224–2242.
[24] L. Santo, K.T. Siu, N. Raje, Targeting cyclin-dependent kinases and cell cycle progression in human cancers, Semin. Oncol. 42 (2015) 788–800.
[25] E.A. Musgrove, C.E. Caldon, J. Barraclough, A. Stone, R.L. Sutherland, Cyclin D as a therapeutic target in cancer, Nat. Rev. Cancer 11 (2011) 558–572.
[26] T. Santarius, J. Shipley, D. Brewer, M.R. Stratton, C.S. Cooper, A census of amplified and overexpressed human cancer genes, Nat. Rev. Cancer 10 (2010) 59–64.
[27] M. Schwaederlé, G.A. Daniels, D.E. Piccioni, P.T. Fanta, R.B. Schwab, K.A. Shimabukuro, et al., Cyclin alterations in diverse cancers: outcome and co-amplification network, Oncotarget 6 (2015) 3033–3042.
[28] P.L. Bergsagel, W.M. Kuehl, F. Zhan, J. Sawyer, B. Barlogie, J. Shaughnessy Jr., Cyclin D dysregulation: an early and unifying pathogenic event in multiple myeloma, Blood 106 (2005) 296–303.
[29] N. Nakayama, K. Nakayama, Y. Shamima, M. Ishikawa, A. Katagiri, K. Iida, et al., Gene amplification *CCNE1* is related to poor survival and potential therapeutic

target in ovarian cancer, Cancer 116 (2010) 2621–2634.
[30] A.M. Karst, P.M. Jones, N. Vena, A.H. Ligon, J.F. Liu, M.S. Hirsch, et al., Cyclin E1 deregulation occurs early in secretory cell transformation to promote formation of fallopian tube-derived high-grade serous ovarian cancers, Cancer Res. 74 (2014) 1141–1152.
[31] E. Kuhn, A. Bahadirli-Talbott, I.M. Shih, Frequent *CCNE1* amplification in endometrial intraepithelial carcinoma and uterine serous carcinoma, Mod. Pathol. 27 (2014) 1014–1019.
[32] H.G. Drexler, Review of alterations of the cyclin-dependent kinase inhibitor INK4 family genes p15, p16, p18 and p19 in human leukemia-lymphoma cells, Leukemia 12 (1998) 845–859.
[33] F. Mendrzyk, B. Radlwimmer, S. Joos, F. Kokocinski, A. Benner, D.E. Stange, et al., Genomic and protein expression profiling identifies CDK6 as novel independent prognostic marker in medulloblastoma, J. Clin. Oncol. 23 (2005) 8853–8862.
[34] U. Asghar, A.K. Witkiewicz, N.C. Turner, E.S. Knudsen, The history and future of targeting cyclin-dependent kinases in cancer therapy, Nat. Rev. Drug Discov. 14 (2015) 130–146.
[35] R.L. Siegel, K.D. Miller, A. Jemal, Cancer statistics, 2018, CA: Cancer J. Clin. (68) (2018) 7–30.
[36] F. Bray, J. Ferlay, I. Soerjomataram, R.L. Siegel, L.A. Torre, A. Jemal, Global cancer statistics 2018: GLOBOCAN estimates of incidence and mortality worldwide for 36 cancers in 185 countries, CA: Cancer J. Clin. 68 (2018) 394–424.
[37] J.L. Wittliff, Steroid-hormone receptors in breast cancer, Cancer 53 (1984) 630–643.
[38] R. Roskoski Jr., ERK1/2 MAP kinases: structure, function, and regulation, Pharmacol. Res. 66 (2012) 105–143.
[39] N.R. Brown, M.E. Noble, J.A. Endicott, L.N. Johnson, The structural basis for specificity of substrate and recruitment peptides for cyclin-dependent kinases, Nat. Cell Biol. 1 (1999) 438–443.
[40] N.R. Brown, S. Korolchuk, M.P. Martin, W.A. Stanley, R. Moukhametzianov, M.E. Noble, et al., CDK1 structures reveal conserved and unique features of the essential cell cycle CDK, Nat. Commun. 6 (2015) 6769.
[41] S.S. Taylor, E. Radzio-Andzelm, T. Hunter, How do protein kinases discriminate between serine/threonine and tyrosine? Structural insights from the insulin receptor protein-tyrosine kinase, FASEB J. 9 (1995) 1255–1266.
[42] S.K. Hanks, T. Hunter, Protein kinases 6. The eukaryotic protein kinase superfamily: kinase (catalytic) domain structure and classification, FASEB J. 9 (1995) 576–596.
[43] D.R. Knighton, J.H. Zheng, L.F. Ten Eyck, V.A. Ashford, N.H. Xuong, S.S. Taylor, et al., Crystal structure of the catalytic subunit of cyclic adenosine monophosphate-dependent protein kinase, Science 253 (1991) 407–414.
[44] D.R. Knighton, J.H. Zheng, L.F. Ten Eyck, N.H. Xuong, S.S. Taylor, J.M. Sowadski, Structure of a peptide inhibitor bound to the catalytic subunit of cyclic adenosine monophosphate-dependent protein kinase, Science 253 (1991) 414–420.
[45] S.S. Taylor, A.P. Kornev, Protein kinases: evolution of dynamic regulatory proteins, Trends Biochem. Sci. 36 (2011) 65–77.
[46] R. Roskoski Jr., A historical overview of protein kinases and their targeted small molecule inhibitors, Pharmacol. Res. 100 (2015) 1–23.
[47] D.M. Jacobsen, Z.Q. Bao, P. O'Brien, C.L. Brooks 3rd, M.A. Young, Price to be paid for two-metal catalysis: magnesium ions that accelerate chemistry unavoidably limit product release from a protein kinase, J. Am. Chem. Soc. 134 (2012) 15357–15370.
[48] R. Roskoski Jr., Src protein-tyrosine kinase structure, mechanism, and small molecule inhibitors, Pharmacol. Res. 94 (2015) 9–25.
[49] J. Zhou, J.A. Adams, Participation of ADP dissociation in the rate-determining step in cAMP-dependent protein kinase, Biochemistry 36 (1997) 15733–15738.
[50] A.P. Kornev, N.M. Haste, S.S. Taylor, L.F. Ten Eyck, Surface comparison of active and inactive protein kinases identifies a conserved activation mechanism, Proc. Natl. Acad. Sci. U. S. A. 103 (2006) 17783–17788.
[51] A.P. Kornev, S.S. Taylor, L.F. Ten Eyck, A helix scaffold for the assembly of active protein kinases, Proc. Natl. Acad. Sci. U. S. A. 105 (2008) 14377–14382.
[52] H.S. Meharena, P. Chang, M.M. Keshwani, K. Oruganty, A.K. Nene, N. Kannan, et al., Deciphering the structural basis of eukaryotic protein kinase regulation, PLoS Biol. 11 (2013) e1001680.
[53] R. Roskoski Jr., Classification of small molecule protein kinase inhibitors based upon the structures of their drug-enzyme complexes, Pharmacol. Res. 103 (2016) 26–48.
[54] R. Roskoski Jr., Anaplastic lymphoma kinase (ALK): structure, oncogenic activation, and pharmacological inhibition, Pharmacol. Res. 68 (2013) 68–94.
[55] R. Roskoski Jr., Anaplastic lymphoma kinase (ALK) inhibitors in the treatment of ALK-driven lung cancers, Pharmacol. Res. 117 (2017) 343–356.
[56] R. Roskoski Jr., Janus kinase (JAK) inhibitors in the treatment of inflammatory and neoplastic diseases, Pharmacol. Res. 111 (2016) 784–803.
[57] R. Roskoski Jr., The role of small molecule Kit protein-tyrosine kinase inhibitors in the treatment of neoplastic disorders, Pharmacol. Res. 133 (2018) 35–52.
[58] R. Roskoski Jr., Allosteric MEK1/2 inhibitors including cobimetanib and trametinib in the treatment of cutaneous melanomas, Pharmacol. Res. 117 (2017) 20–31.
[59] R. Roskoski Jr., The role of small molecule platelet-derived growth factor receptor (PDGFR) inhibitors in the treatment of neoplastic disorders, Pharmacol. Res. 129 (2018) 65–83.
[60] R. Roskoski Jr., RAF protein-serine/threonine kinases: structure and regulation, Biochem. Biophys. Res. Commun. 399 (2010) 313–317.
[61] R. Roskoski Jr., Targeting oncogenic Raf protein-serine/threonine kinases in human cancers, Pharmacol. Res. 135 (2018) 239–258.
[62] R. Roskoski Jr., A. Sadeghi-Nejad, Role of RET protein-tyrosine kinase inhibitors in the treatment RET-driven thyroid and lung cancers, Pharmacol. Res. 128 (2018) 1–17.
[63] R. Roskoski Jr., ROS1 protein-tyrosine kinase inhibitors in the treatment of ROS1 fusion protein-driven non-small cell lung cancers, Pharmacol. Res. 121 (2017) 202–212.
[64] R. Roskoski Jr., Small molecule inhibitors targeting the EGFR/ErbB family of protein-tyrosine kinases in human cancers, Pharmacol. Res. 139 (2019) xxx–xxx.
[65] R. Roskoski Jr., Vascular endothelial growth factor (VEGF) and VEGF receptor inhibitors in the treatment of renal cell carcinomas, Pharmacol. Res. 120 (2017) 116–132.
[66] K. Shah, Y. Liu, C. Deirmengian, K.M. Shokat, Engineering unnatural nucleotide specificity for Rous sarcoma virus tyrosine kinase to uniquely label its direct substrates, Proc. Natl. Acad. Sci. U. S. A. 94 (1997) 3565–3570.
[67] Y. Liu, K. Shah, F. Yang, L. Witucki, K.M. Shokat, A molecular gate which controls unnatural ATP analogue recognition by the tyrosine kinase v-Src, Bioorg. Med. Chem. Lett. 6 (1998) 1219–1226.
[68] A.C. Dar, K.M. Shokat, The evolution of protein kinase inhibitors from antagonists to agonists of cellular signaling, Annu. Rev. Biochem. 80 (2011) 769–795.
[69] F. Zuccotto, E. Ardini, E. Casale, M. Angiolini, Through the "gatekeeper door": exploiting the active kinase conformation, J. Med. Chem. 53 (2010) 2691–2694.
[70] L.K. Gavrin, E. Saiah, Approaches to discover non-ATP site inhibitors, Med. Chem. Commun. 4 (2013) 41.
[71] V. Lamba, I. Ghosh, New directions in targeting protein kinases: focusing upon true allosteric and bivalent inhibitors, Curr. Pharm. Des. 18 (2012) 2936–2945.
[72] R.S. Vijayan, P. He, V. Modi, K.C. Duong-Ly, H. Ma, J.R. Peterson, et al., Conformational analysis of the DFG-out kinase motif and biochemical profiling of structurally validated type II inhibitors, J. Med. Chem. 58 (2015) 466–479.
[73] F.E. Kwarcinski, K.R. Brandvold, S. Phadke, O.M. Beleh, T.K. Johnson, J.L. Meagher, et al., Conformation-selective analogues of dasatinib reveal insight into kinase inhibitor binding and selectivity, ACS Chem. Biol. 11 (2016) 1296–1304.
[74] Z. Zhao, H. Wu, L. Wang, Y. Liu, S. Knapp, Q. Liu, N.S. Gray, Exploration of type II binding mode: A privileged approach for kinase inhibitor focused drug discovery? ACS Chem. Biol. 9 (2014) 1230–1241.
[75] P.M. Ung, R. Rahman, A. Schlessinger, Redefining the protein kinase conformational space with machine learning, Cell Chem. Biol. 25 (2018) 916-24.e2.
[76] J.J. Liao, Molecular recognition of protein kinase binding pockets for design of potent and selective kinase inhibitors, J. Med. Chem. 50 (2007) 409–424.
[77] O.P. van Linden, A.J. Kooistra, R. Leurs, I.J. de Esch, C. de Graaf, KLIFS: a knowledge-based structural database to navigate kinase-ligand interaction space, J. Med. Chem. 57 (2014) 249–277.
[78] A.J. Kooistra, A. Volkamer, Kinase-centric computational drug development, Ann. Rep. Med. Chem. 50 (2017) 197–236.
[79] D. Bajusz, G.G. Ferenczy, G.M. Keserá, Structure-based virtual screening approaches in kinase-directed drug discovery, Curr. Top. Med. Chem. 17 (2017) 2235–2259.
[80] D. Fabbro, S.W. Cowan-Jacob, H. Moebitz, Ten things you should know about protein kinases: IUPHAR Review 14, Br. J. Pharmacol. 172 (2015) 2675–2700.
[81] P.M. Fischer, Approved and experimental small-molecule oncology kinase inhibitor drugs: a mid-2016 overview, Med. Res. Rev. 37 (2017) 314–367.
[82] F. Carles, S. Bourg, C. Meyer, P. Bonnet, PKIDB: a curated, annotated and updated database of protein kinase inhibitors in clinical trials, Molecules 23 (2018), https://doi.org/10.3390/molecules23040908.
[83] R.S. Finn, J.P. Crown, I. Lang, K. Boer, I.M. Bondarenko, S.O. Kulyk, et al., The cyclin-dependent kinase 4/6 inhibitor palbociclib in combination with letrozole versus letrozole alone as first-line treatment of oestrogen receptor-positive, HER2-negative, advanced breast cancer (PALOMA-1/TRIO-18): a randomised phase 2 study, Lancet Oncol. 16 (2015) 25–35.
[84] R.S. Finn, M. Martin, H.S. Rugo, S. Jones, S.A. Im, K. Gelmon, et al., Palbociclib and letrozole in advanced breast cancer, N. Engl. J. Med. 375 (2016) 1925–1936.
[85] B. O'Leary, R.S. Finn, N.C. Turner, Treating cancer with selective CDK4/6 inhibitors, Nat. Rev. Clin. Oncol. 13 (2016) 417–430.
[86] N.C. Turner, D.J. Slamon, J. Ro, I. Bondarenko, S.A. Im, N. Masuda, et al., Overall survival with palbociclib and fulvestrant in advanced breast cancer, N. Engl. J. Med. 379 (2018) 1926–1936.
[87] D.W. Fry, P.J. Harvey, P.R. Keller, W.L. Elliott, M. Meade, E. Trachet, et al., Specific inhibition of cyclin-dependent kinase 4/6 by PD 0332991 and associated antitumor activity in human tumor xenografts, Mol. Cancer Ther. 3 (2004) 1427–1438.
[88] S.N. VanderWel, P.J. Harvey, D.J. McNamara, J.T. Repine, P.R. Keller, J. Quin 3rdet al., Pyrido[2,3-d]pyrimidin-7-ones as specific inhibitors of cyclin-dependent kinase 4, J. Med. Chem. 48 (2005) 2371–2387.
[89] P.L. Toogood, P.J. Harvey, J.T. Repine, D.J. Sheehan, S.N. VanderWel, H. Zhou, et al., Discovery of a potent and selective inhibitor of cyclin-dependent kinase 4/6, J. Med. Chem. 48 (2005) 2388–2406.
[90] G.N. Hortobagyi, S.M. Stemmer, H.A. Burris, Y.S. Yap, G.S. Sonke, S. Paluch-Shimon, et al., Ribociclib as first-line therapy for HR-Positive, advanced breast Cancer, N. Engl. J. Med. 375 (2016) 1738–1748.
[91] G.N. Hortobagyi, S.M. Stemmer, H.A. Burris, Y.S. Yap, G.S. Sonke, S. Paluch-Shimon, et al., Updated results from MONALEESA-2, a phase III trial of first-line ribociclib plus letrozole versus placebo plus letrozole in hormone receptor-positive, HER2-negative advanced breast cancer, Ann. Oncol. 29 (2018) 1541–1547.
[92] A. Shah, E. Bloomquist, S. Tang, W. Fu, Y. Bi, Q. Liu, et al., FDA approval: ribociclib for the treatment of postmenopausal women with hormone receptor-positive, HER-negative advanced or metastatic breast cancer, Clin. Cancer Res. 24 (2018) 2999–3004.

[93] J. O'Shaughnessy, K. Petrakova, G.S. Sonke, P. Conte, C.L. Arteaga, D.A. Cameron, et al., Ribociclib plus letrozole versus letrozole alone in patients with de novo HR+, HER2- advanced breast cancer in the randomized MONALEESA-2 trial, Breast Cancer Res. Treat. 168 (2018) 127–134.
[94] C.J. Sherr, D. Beach, G.I. Shapiro, Targeting CDK4 and CDK6: from discovery to therapy, Cancer Discov. 6 (2016) 353–367.
[95] L. Manso, O.C. Freedman, G. Garnica Jaliffe, T. Forrester, M. Frenzel, S. Barriga, et al., MONARCH 3: abemaciclib as initial therapy for advanced breast Cancer, J. Clin. Oncol. 35 (2017) 3638–3646.
[96] G.W. Sledge Jr., M. Toi, P. Neven, J. Sohn, K. Inoue, X. Pivot, et al., MONARCH 2: abemaciclib in combination with fulvestrant in women with HR+/HER2- advanced breast cancer who had progressed while receiving endocrine therapy, J. Clin. Oncol. 35 (2017) 2875–2884.
[97] A. Palumbo, J. Lau, M. Saraceni, Abemaciclib: the newest cdk4/6 inhibitor for the treatment of breast cancer, Ann. Pharmacother. (2018) 1060028018795146.
[98] J.M. Martin, L.J. Goldstein, Profile of abemaciclib and its potential in the treatment of breast cancer, Onco. Ther. 11 (2018) 5253–5259.
[99] Y. Wang, W.J. Liu, L. Yin, H. Li, Z.H. Chen, D.X. Zhu, et al., Design and synthesis of 4-(2,3-dihydro-1H-benzo[d]pyrrolo[1,2-a]imidazol-7-yl)-N-(5-(piperazin-1-ylmethyl)pyridine-2-yl)pyrimidin-2-amine as a highly potent and selective cyclin-dependent kinases 4 and 6 inhibitors and the discovery of structure-activity relationships, Bioorg. Med. Chem. Lett. 28 (2018) 974–978.
[100] S. George, B.S. Kasimis, J. Cogswell, P. Schwarzenberger, G.I. Shapiro, P. Fidias, et al., Phase I study of flavopiridol in combination with paclitaxel and carboplatin in patients with non-small-cell lung cancer, Clin. Lung Cancer 9 (2008) 160–165.
[101] T.S. Lin, A.S. Ruppert, A.J. Johnson, B. Fischer, N.A. Heerema, L.A. Andritsos, et al., Phase II study of flavopiridol in relapsed chronic lymphocytic leukemia demonstrating high response rates in genetically high-risk disease, J. Clin. Oncol. 27 (2009) 6012–6018.
[102] J.E. Karp, B.D. Smith, L.S. Resar, J.M. Greer, A. Blackford, M. Zhao, et al., Phase 1 and pharmacokinetic study of bolus-infusion flavopiridol followed by cytosine arabinoside and mitoxantrone for acute leukemias, Blood 117 (2011) 3302–3310.
[103] J.F. Zeidner, M.C. Foster, A.L. Blackford, M.R. Litzow, L.E. Morris, S.A. Strickland, et al., Randomized multicenter phase II study of flavopiridol (alvocidib), cytarabine, and mitoxantrone (FLAM) versus cytarabine/daunorubicin (7+3) in newly diagnosed acute myeloid leukemia, Haematologica 100 (2015) 1172–1179.
[104] M.C. Lanasa, L. Andritsos, J.R. Brown, J. Gabrilove, F. Caligaris-Cappio, P. Ghia, et al., Final results of EFC6663: a multicenter, international, phase 2 study of alvocidib for patients with fludarabine-refractory chronic lymphocytic leukemia, Leuk. Res. 39 (2015) 495–500.
[105] K. Paruch, M.P. Dwyer, C. Alvarez, C. Brown, T.Y. Chan, R.J. Doll, et al., Discovery of dinaciclib (SCH 727965): a potent and selective inhibitor of cyclin-dependent kinases, ACS Med. Chem. Lett. 1 (2010) 204–208.
[106] D. Parry, T. Guzi, F. Shanahan, N. Davis, D. Prabhavalkar, D. Wiswell, et al., Dinaciclib (SCH 727965), a novel and potent cyclin-dependent kinase inhibitor, Mol. Cancer Ther. 9 (2010) 2344–2353.
[107] J.J. Nemunaitis, K.A. Small, P. Kirschmeier, D. Zhang, Y. Zhu, Y.M. Jou, et al., A first-in-human, phase 1, dose-escalation study of dinaciclib, a novel cyclin-dependent kinase inhibitor, administered weekly in subjects with advanced malignancies, J. Transl. Med. 11 (2013) 259.
[108] J.J. Stephenson, J. Nemunaitis, A.A. Joy, J.C. Martin, Y.M. Jou, D. Zhang, et al., Randomized phase 2 study of the cyclin-dependent kinase inhibitor dinaciclib (MK-7965) versus erlotinib in patients with non-small cell lung cancer, Lung Cancer 83 (2014) 219–223.
[109] M.M. Mita, A.A. Joy, A. Mita, K. Sankhala, Y.M. Jou, D. Zhang, et al., Randomized phase II trial of the cyclin-dependent kinase inhibitor dinaciclib (MK-7965) versus capecitabine in patients with advanced breast cancer, Clin. Breast Cancer 14 (2014) 169–176.
[110] J. Flynn, J. Jones, A.J. Johnson, L. Andritsos, K. Maddocks, S. Jaglowski, et al., Dinaciclib is a novel cyclin-dependent kinase inhibitor with significant clinical activity in relapsed and refractory chronic lymphocytic leukemia, Leukemia 29 (2015) 1524–1529.
[111] Z. Mitri, C. Karakas, C. Wei, B. Briones, H. Simmons, N. Ibrahim, et al., A phase 1 study with dose expansion of the CDK inhibitor dinaciclib (SCH 727965) in combination with epirubicin in patients with metastatic triple negative breast cancer, Invest. New Drugs 33 (2015) 890–894.
[112] U. Lücking, R. Jautelat, M. Krüger, T. Brumby, P. Lienau, M. Schäfer, et al., The lab oddity prevails: discovery of pan-CDK inhibitor (R)-S-cyclopropyl-S-(4-{[4-{[(1R,2R)-2-hydroxy-1-methylpropyl]oxy}-5-(trifluoromethyl)pyrimidin-2-yl]amino}phenyl)sulfoximide (BAY 1000394) for the treatment of cancer, ChemMedChem 8 (2013) 1067–1085.
[113] P. Ayaz, D. Andres, D.A. Kwiatkowski, C.C. Kolbe, P. Lienau, G. Siemeister, et al., Conformational adaption may explain the slow dissociation kinetics of roniciclib (BAY 1000394), a type I CDK inhibitor with kinetic selectivity for CDK2 and CDK9, ACS Chem. Biol. 11 (2016) 1710–1719.
[114] R. Bahleda, J.E. Grilley-Olson, R. Govindan, F. Barlesi, L. Greillier, M. Perol, et al., Phase I dose-escalation studies of roniciclib, a pan-cyclin-dependent kinase inhibitor, in advanced malignancies, Br. J. Cancer 116 (2017) 1505–1512.
[115] S. He, P.J. Roberts, J.A. Sorrentino, J.E. Bisi, H. Storrie-White, R.G. Tiessen, et al., Transient CDK4/6 inhibition protects hematopoietic stem cells from chemotherapy-induced exhaustion, Sci. Transl. Med. 9 (2017) pii: eaal3986.
[116] S. Parylo, A. Vennepureddy, V. Dhar, P. Patibandla, A. Sokoloff, Role of cyclin-dependent kinase 4/6 inhibitors in the current and future eras of cancer treatment, J. Oncol. Pharm. Pract. (2018) 1078155218770904.
[117] J.E. Bisi, J.A. Sorrentino, P.J. Roberts, F.X. Tavares, J.C. Strum, Preclinical characterization of G1T28: a novel CDK4/6 inhibitor for reduction of chemotherapy-induced myelosuppression, Mol. Cancer Ther. 15 (2016) 783–793.
[118] L. Santo, S. Vallet, T. Hideshima, D. Cirstea, H. Ikeda, S. Pozzi, et al., AT7519, A novel small molecule multi-cyclin-dependent kinase inhibitor, induces apoptosis in multiple myeloma via GSK-3β activation and RNA polymerase II inhibition, Oncogene 29 (2010) 2325–2336.
[119] D. Mahadevan, R. Plummer, M.S. Squires, D. Rensvold, S. Kurtin, C. Pretzinger, et al., A phase I pharmacokinetic and pharmacodynamic study of AT7519, a cyclin-dependent kinase inhibitor in patients with refractory solid tumors, Ann. Oncol. 22 (2011) 2137–2143.
[120] E.X. Chen, S. Hotte, H. Hirte, L.L. Siu, J. Lyons, M. Squires, et al., A Phase I study of cyclin-dependent kinase inhibitor, AT7519, in patients with advanced cancer: NCIC Clinical Trials Group IND 177, Br. J. Cancer 111 (2014) 2262–2267.
[121] M.D. Seftel, J. Kuruvilla, T. Kouroukis, V. Banerji, G. Fraser, M. Crump, et al., The CDK inhibitor AT7519M in patients with relapsed or refractory chronic lymphocytic leukemia (CLL) and mantle cell lymphoma. A Phase II study of the Canadian Cancer Trials Group, Leuk. Lymphoma 58 (2017) 1358–1365.
[122] P. Eliades, D.M. Miller, B. Miao, R. Kumar, M. Taylor, S. Buch, et al., A novel multi-CDK inhibitor P1446A-05 restricts melanoma growth and produces synergistic effects in combination with MAPK pathway inhibitors, Cancer Biol. Ther. 17 (2016) 778–784.
[123] J. Dey, T.L. Deckwerth, W.S. Kerwin, J.R. Casalini, A.J. Merrell, M.O. Grenley, et al., Voruciclib, a clinical stage oral CDK9 inhibitor, represses MCL-1 and sensitizes high-risk Diffuse Large B-cell Lymphoma to BCL2 inhibition, Sci. Rep. 71 (2017) 18007.
[124] P. Gupta, Y.K. Zhang, X.Y. Zhang, Y.J. Wang, K.W. Lu, T. Hall, et al., Voruciclib, a potent CDK4/6 inhibitor, antagonizes ABCB1 and ABCG2-Mediated multi-drug resistance in Cancer cells, Cell. Physiol. Biochem. 45 (2018) 1515–1528.
[125] J. Wang, Q. Li, J. Yuan, J. Wang, Z. Chen, Z. Liu, Z. Li, et al., CDK4/6 inhibitor-SHR6390 exerts potent antitumor activity in esophageal squamous cell carcinoma by inhibiting phosphorylated Rb and inducing G1 cell cycle arrest, J. Transl. Med. 15 (2017) 127.
[126] A. Burgess, J. Vuong, S. Rogers, M. Malumbres, S.I. O'Donoghue, SnapShot: phosphoregulation of mitosis, Cell 169 (2017) 1358–1358.e1.
[127] K. Nasmyth, A prize for proliferation, Cell 107 (2001) 689–701.
[128] L.H. Hartwell, J. Culotti, B. Reid, Genetic control of the cell-division cycle in yeast. I. Detection of mutants, Proc. Natl. Acad. Sci. U. S. A. 66 (1970) 352–359.
[129] P. Nurse, Genetic control of cell size at cell division in yeast, Nature 256 (1975) 547–551.
[130] T. Evans, E.T. Rosenthal, J. Youngblom, D. Distel, T. Hunt, Cyclin: a protein specified by maternal mRNA in sea urchin eggs that is destroyed at each cleavage division, Cell 33 (1983) 389–396.
[131] H. Rajagopalan, C. Lengauer, Aneuploidy and cancer, Nature 432 (2004) 338–341.
[132] A.M. Senderowicz, E.A. Sausville, Preclinical and clinical development of cyclin-dependent kinase modulators, J. Natl. Cancer Inst. 92 (2000) 376–387.
[133] G. Kaur, M. Stetler-Stevenson, S. Sebers, P. Worland, H. Sedlacek, C. Myers, et al., Growth inhibition with reversible cell cycle arrest of carcinoma cells by flavone L86-8275, J. Natl. Cancer Inst. 84 (1992) 1736–1740.
[134] C. Guarducci, M. Bonechi, G. Boccalini, M. Benelli, E. Risi, A. Di Leo, et al., Mechanisms of resistance to CDK4/6 inhibitors in breast Cancer and potential biomarkers of response, Breast Care (Basel) 12 (2017) 304–308.
[135] F. Lynce, A.N. Shajahan-Haq, S.M. Swain, CDK4/6 inhibitors in breast cancer therapy: current practice and future opportunities, Pharmacol. Ther. 191 (2018) 65–73.
[136] E.S. Knudsen, A.K. Witkiewicz, The strange case of CDK4/6 inhibitors: mechanisms, resistance, and combination strategies, Trends Cancer 3 (2017) 39–55.
[137] C. Yang, Z. Li, T. Bhatt, M. Dickler, D. Giri, M. Scaltriti, et al., Acquired CDK6 amplification promotes breast cancer resistance to CDK4/6 inhibitors and loss of ER signaling and dependence, Oncogene 36 (2017) 2255–2264.
[138] D. Ribnikar, S.R. Volovat, F. Cardoso, Targeting CDK4/6 pathways and beyond in breast cancer, Breast 43 (2018) 8–17.
[139] R. Roskoski Jr., Guidelines for preparing color figures for everyone including the colorblind, Erratum in: Pharmacol. Res. 119 (2017) 240–241, https://doi.org/10.1016/j.phrs.2018.09.019.